Applied Microbiology and Biotechnology (2024) 108:50
https://doi.org/10.1007/s00253-023-12885-7

BIOTECHNOLOGICAL PRODUCTS AND PROCESS ENGINEERING

High-level biosynthesis of enantiopure germacrene D in yeast

Shubha Sharma[1,2] · Seema Chaurasia[1] · Sandeep Dinday[1,3] · Gaurav Srivastava[1] · Anamika Singh[1] · Chandan Singh Chanotiya[2,4] · Sumit Ghosh[1,2]

Received: 22 June 2023 / Revised: 18 September 2023 / Accepted: 30 September 2023

Abstract

Germacrene D, a sesquiterpenoid compound found mainly in plant essential oils at a low level as (+) and/or (−) enantiomeric forms, is an ingredient for the fragrance industry, but a process for the sustainable supply of enantiopure germacrene D is not yet established. Here, we demonstrate metabolic engineering in yeast (*Saccharomyces cerevisiae*) achieving biosynthesis of enantiopure germacrene D at a high titer. To boost farnesyl pyrophosphate (FPP) flux for high-level germacrene D biosynthesis, a background yeast chassis (CENses5C) was developed by genomic integration of the expression cassettes for eight ergosterol pathway enzymes that sequentially converted acetyl-CoA to FPP and by replacing squalene synthase promoter with a copper-repressible promoter, which restricted FPP flux to the competing pathway. Galactose-induced expression of codon-optimized plant germacrene D synthases led to 13–30 fold higher titers of (+) or (−)-germacrene D in CENses5C than the parent strain CEN.PK2.1C. Furthermore, genomic integration of germacrene D synthases in *GAL80*, *LPP1* and *rDNA* loci generated CENses8(+D) and CENses8(−D) strains, which produced 41.36 µg/ml and 728.87 µg/ml of (+) and (−)-germacrene D, respectively, without galactose supplementation. Moreover, coupling of mitochondrial citrate pool to the cytosolic acetyl-CoA, by expressing a codon-optimized ATP-citrate lyase of oleaginous yeast, resulted in 137.71 µg/ml and 815.81 µg/ml of (+) or (−)-germacrene D in CENses8(+D)* and CENses8(−D)* strains, which were 67–120 fold higher titers than in CEN.PK2.1C. In fed-batch fermentation, CENses8(+D)* and CENses8(−D)* produced 290.28 µg/ml and 2519.46 µg/ml (+) and (−)-germacrene D, respectively, the highest titers in shake-flask fermentation achieved so far.

Key points

- *Engineered S. cerevisiae produced enantiopure (+) and (−)-germacrene D at high titers*
- *Engineered strain produced up to 120-fold higher germacrene D than the parental strain*
- *Highest titers of enantiopure (+) and (−)-germacrene D achieved so far in shake-flask*

Keywords Sesquiterpenoid · Germacrene D · Enantiomer · *Saccharomyces cerevisiae* · ERG pathway · Metabolic engineering

Shubha Sharma and Seema Chaurasia contributed equally to this work.

✉ Sumit Ghosh
sumitghosh@cimap.res.in

1 Plant Biotechnology Division, Council of Scientific and Industrial Research-Central Institute of Medicinal and Aromatic Plants (CSIR-CIMAP), Lucknow 226015, India

2 Academy of Scientific and Innovative Research (AcSIR), Ghaziabad 201002, India

3 Present Address: School of Agricultural Biotechnology, Punjab Agricultural University, Ludhiana 141004, India

4 Phytochemistry Division, Council of Scientific and Industrial Research-Central Institute of Medicinal and Aromatic Plants (CSIR-CIMAP), Lucknow 226015, India

Introduction

Germacrenes are the volatile sesquiterpenes (C15 monocyclic isoprenoids) typically produced in plants by the sesquiterpene synthases (sesqui-TPSs) using the acyclic precursor farnesyl pyrophosphate (FPP). Several structural isomers of germacrenes (germacrene A–E) were identified in plants; however, germacrene A and D were most frequently detected (Adio 2009; Cascón et al. 2012). Germacrene A and D were both suggested to protect plants against pathogenic microbes and showed a deterrent effect on insects such as mosquitoes, aphids, and ticks, while attracting pollinating insects by acting as pheromones (Schmidt et al. 1999; Stranden et al. 2003). Notably, germacrene D is listed as an ingredient for

Published online: 06 January 2024

the fragrance industry by the International Fragrance Association (https://ifrafragrance.org/). Germacrene D is also a key intermediate in the semi-synthesis of several classes of sesquiterpenoids such as selinene, elemane, amorphene, muurolene, cadinene, oppositane, axane, and isodaucane, thus making it relevant for industrial production (Yoshihara et al. 1969; Bülow and König 2000; Faraldos et al. 2007).

Germacrene D is mainly detected in low quantity as an essential oil component in plants such as *Solidago canadensis*, *Ocimum* species, *Hypericum perforatum*, *Croton ferrugineus*, and *Bursera* species (Chanotiya and Yadav 2008; Mockute et al. 2008; Noge and Becerra 2009; Rana and Blázquez 2015; Valarezo et al. 2021). However, *S. canadensis* essential oil is particularly rich in germacrene D, which accounts for up to 75% of essential oil components (Chanotiya and Yadav 2008). Typically, germacrene D exists in two chiral forms, *S*-(−)-germacrene D and *R*-(+)-germacrene D, and depending on which enantiospecific sesqui-TPS (germacrene D synthase) is expressed, plants generally produce only one of these enantiomers (Adio 2009; Casiglia et al. 2017). (−)-Germacrene D is mainly produced in higher plants, while (+)-germacrene D is found in lower plants such as liverworts. However, one of the exceptions to this notion was reported in *S. canadensis*, which was shown to express two enantio-specific germacrene D synthases (Sc11 and Sc19) and thus contained both the enantiomeric forms of germacrene D (Bülow and König 2000; Steliopoulos et al. 2002; Prosser et al. 2004). Interestingly, insects responded with high sensitivity and selectivity to (−)-germacrene D than (+)-germacrene D, suggesting that enantiomers might differ in bioactivities (Stranden et al. 2002, 2003). Nonetheless, isolating enantiopure germacrene D from the plants can be tricky due to the high sensitivity to acidic pH and high temperature and poor yield (Faraldos et al. 2007).

Due to the ease of genetic manipulation and scalability, microorganisms can enable the production of stereochemically pure terpenoids with high product yield (Paddon et al. 2013; Meadows et al. 2016; Ma et al. 2021; Cao et al. 2022; Bureau et al. 2023). Stereoisomers are generally produced by distinct TPSs in natural hosts (Christianson 2017). Hence, heterologous expression of terpene synthases can ensure the biosynthesis of stereochemically pure products. While there were reports on the production of germacrene A in yeast (*Saccharomyces cerevisiae)* (Hu et al. 2017; Bröker et al. 2020; Zhang et al. 2021), but, no such studies have been carried out for germacrene D until very recently (Liu et al. 2022). The yeast-based biosynthetic platform for (−)-germacrene D required galactose as an inducer of gene expression and high titer production of (+)-germacrene D was not explored (Liu et al. 2022). The constitutive production platform of enantiopure germacrene D at a high titer would help to reduce input costs in industrial production. Therefore, the main goal of the present study was to develop a yeast (*S. cerevisiae*) strain that will be suitable for high-level production of enantiopure germacrene D. FPP is formed in *S. cerevisiae* as an intermediate of ergosterol (ERG) pathway, which can be converted to (+) or (−)-germacrene D by expressing enantio-specific germacrene D synthase (Fig. 1). Previous studies showed high-level biosynthesis of FPP-derived metabolites in *S. cerevisiae* following ERG pathway engineering (Paddon et al. 2013; Siemon et al. 2020; Cao et al. 2022). In order to ensure an adequate supply of FPP for sesquiterpene biosynthesis in *S. cerevisiae*, pre-FPP and post-FPP steps of the ERG pathway were modulated (Fig. 1). Particularly, the ERG genes involved in the pre-FPP steps were overexpressed. These genes are *ERG10* (acetyl-CoA C-acetyltransferase), *ERG13* (hydroxylmethylglutaryl-CoA synthase), *HMG1* (3-hydroxy-3-methylglutaryl-coenzyme A reductase), *ERG12* (mevalonate kinase), *ERG8* (phosphomevalonate kinase), *ERG19* (diphosphomevalonate decarboxylase), *IDI* (isopentenyl diphosphate isomerase), and *ERG20* (FPP synthase), which encode the enzymes responsible for the production of FPP from acetyl-CoA in ERG pathway (Fig. 1). Moreover, it was known that the activity of HMG1, a rate-limiting enzyme in the ERG pathway, is controlled by feedback regulation that works post-transcriptionally. The over-expression of tHMG1 (a truncated HMG1 devoid of N-terminal regulatory domain) was found to eliminate the feedback inhibition of HMG1 and resulted in upregulation of the ERG pathway (Donald et al. 1997). This approach was useful in enhancing terpenoid production in *S. cerevisiae*, for example artemisinic acid, taxadiene, patchoulol, and oleanolic acid (Engels et al. 2008; Asadollahi et al. 2008; Paddon et al. 2013; Zhao et al. 2018; Dinday and Ghosh, 2023). Moreover, the post-FPP step of the ERG pathway was repressed to restrict FPP for utilization for ergosterol biosynthesis, so that FPP flux would be efficiently diverted towards sesquiterpene biosynthesis (Paddon et al. 2013; Deng et al. 2022). In ERG pathway, squalene synthase (ERG9) catalyzes the conversion of FPP into squalene, which is finally converted to ergosterol through a series of enzymatic steps (Veen et al. 2003). The endogenous promoter of the *ERG9* was replaced with a copper (P_{CTR3}), methionine (P_{MET3}) or glucose (P_{HXT1}) responsive promoter for the repression of post-FPP step of the ERG pathway (Paddon et al. 2013; Liu et al. 2022). Overall, these metabolic engineering strategies were found to be effective in the high-level production of sesquiterpenes in yeast such as artemisinic acid, (−)-eremophilene, and (+)-valencene (Paddon et al. 2013; Cao et al. 2022; Deng et al. 2022).

Here, we report high-level biosynthesis of (+) and (−)-germacrene D by expressing codon-optimized germacrene D synthases (*Sc11* and *Sc19*) of *S. canadensis* in engineered yeast (*S. cerevisiae*), which does not require an inducer of gene expression, and thus the biosynthetic platform is constitutive. The yeast strain CEN.PK2-1C was used

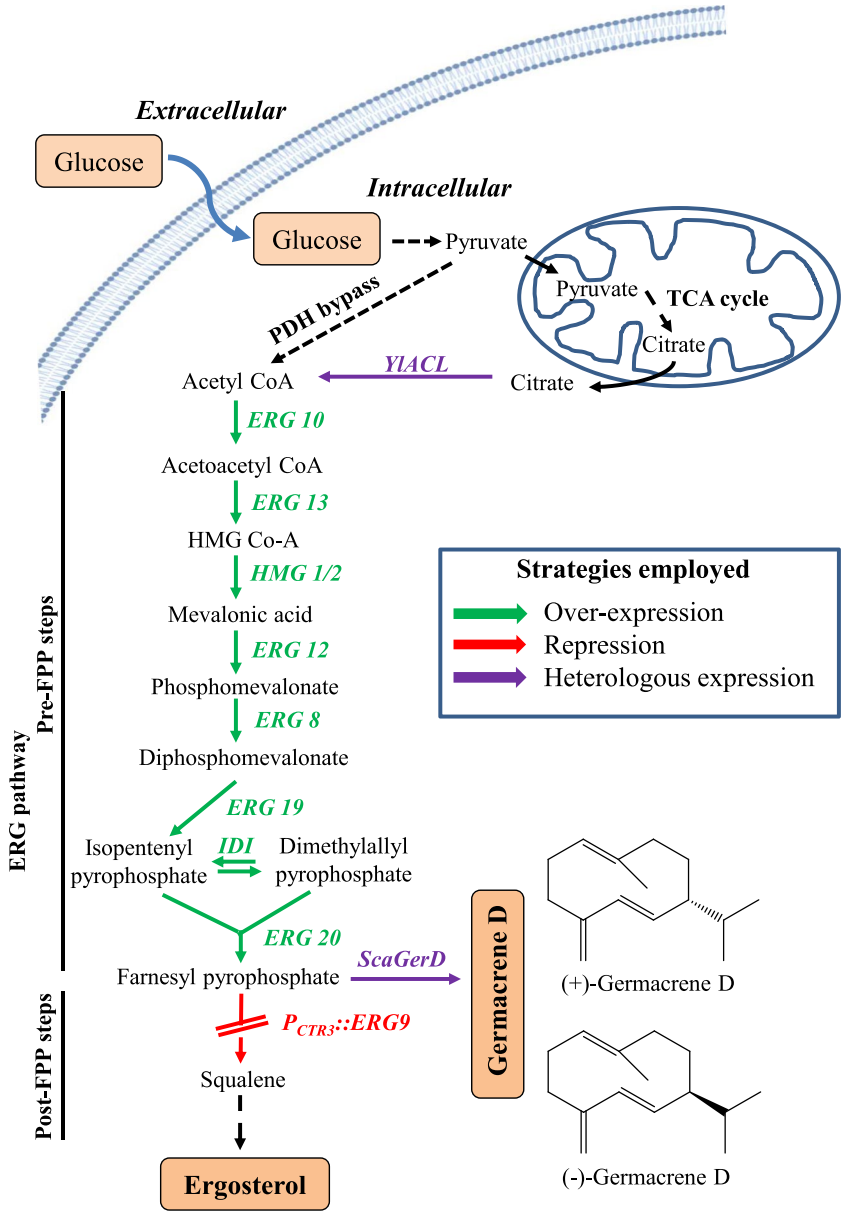

Fig. 1 A schematic biosynthetic pathway displaying the strategies employed to produce enantiopure germacrene D in the engineered *Saccharomyces cerevisiae*. To increase terpenoid precursor flux towards farnesyl pyrophosphate (FPP), eight ERG genes (*ERG10*, *ERG13*, *tHMG1*, *ERG12*, *ERG8*, *ERG19*, *IDI*, and *ERG20*) and codon optimized *Yarrowia lipolytica* ATP-citrate lyase (*YlACL*) were overexpressed, while *ERG9* promoter was replaced with a copper-repressible promoter P_{CTR3}. Codon optimized germacrene D synthase (*ScaGerD*) of *Solidago canadensis* was over-expressed to convert FPP to (+) or (−) germacrene D

as the parent strain in this study because it displayed higher concentrations of lanosterol, ergosterol, and ergosteryl esters during growth on glucose, which suggested increased carbon flux towards the ERG pathway (Daum et al. 1999). Moreover, the selection of CEN.PK2-1C strain for metabolic engineering was also due to its well characterized physiology and an established method for genomic modification (Westfall et al. 2012). To develop the yeast-producing enantiopure germacrene D in a constitutive manner, targeted genomic modifications were carried out in eight loci. Overall, these genomic modifications represented the deletion of two yeast genes (*GAL80* and *LPP1*), over-expression of eight ERG pathway genes (*ERG10*, *ERG13*, *tHMG1*, *ERG12*, *ERG8*, *ERG19*, *IDI*, and *ERG20*), replacement of squalene synthase (*ERG9*) promoter with a copper regulated promoter (P_{CTR3}) and multiple copy integrations of germacrene D synthase expression cassette at *GAL80*, *LPP1*, and *rDNA* loci. This comprehensive metabolic engineering strategy coupled with the expression of a codon-optimized *Yarrowia lipolytica* ATP-citrate lyase (*YlACL*) led to the highest titers of (+)-germacrene D (290.28 µg/ml) and (−)-germacrene D (2519.46 µg/ml) achieved so far in shake-flask.

Materials and methods

Yeast strains, plasmids and media composition

Yeast (*S. cerevisiae*) strains and plasmids used in the work are listed in Table 1. *S. cerevisiae* strains were grown in

Table 1 Plasmids and strains used in this study

Plasmids and strains	Description and genotypes	Sources
Plasmids		
pESC	Yeast episomal plasmid	Agilent Technologies
pYES2/NTB	Yeast episomal plasmid	Invitrogen Life Technologies
pUG6	loxP-P_{AgTEF1}-*kanMX*-T_{AgTEF1}-loxP	Euroscarf
pUG72	loxP-P_{KlURA3}-*KlURA3*-T_{KlURA3}-loxP	Euroscarf
pUG27	loxP-P_{AgTEF1}-*SpHIS5*-T_{AgTEF1}-loxP	Euroscarf
pUG73	loxP-P_{KlLEU2}-*KlLEU2*-T_{KlLEU2}-loxP	Euroscarf
pSH63	Cre-expressing (*pGAL1-cre*) *CEN/ARS* plasmid	Euroscarf
pESC-*ERG10-ERG13*	pESC-HIS,T_{ADH1}-*ERG10*-P_{GAL10}-P_{GAL1}-*ERG13*-T_{CYC1}	This study
pESC-*ERG19-IDI*	pESC-URA,T_{ADH1}-*ERG19*-P_{GAL10}-P_{GAL1}-*IDI*-T_{CYC1}	This study
pESC-*ERG12-ERG8*	pESC-LEU,T_{ADH1}-*ERG12*-P_{GAL10}-P_{GAL1}- *ERG8*-T_{CYC1}	This study
pESC-*ERG20-tHMG1*	pESC-LEU, T_{ADH1}-*ERG20*-P_{GAL10}-P_{GAL1}-*tHMG1*-T_{CYC1}	This study
pYES2-*ScaGerD(+)*	pYES2/NTB, P_{GAL1}-*ScaGerD(+)*-T_{CYC1}	This study
pYES2-*ScaGerD(−)*	pYES2/NTB, P_{GAL1}-*ScaGerD(−)*-T_{CYC1}	This study
pESC-*YlACL1-2*	pESC-TRP, T_{ADH1}-*YlACL2*-P_{GAL10}-P_{GAL1}-*YlACL1*-T_{CYC1}	This study
Strains		
CEN0	CEN.PK2-1C (*MATa*; *ura3-52*; *trp1-289*; *leu2-3,112*; *his3Δ1*; *MAL2-8^C*; *SUC2*)	Euroscarf
CEN0(+D)	CEN0, expressing pYES2-*ScaGerD(+)*	This study
CEN0(−D)	CEN0, expressing pYES2-*ScaGerD(−)*	This study
CENses1	CEN0, *lys5*:: loxP-P_{AgTEF1}-*kanMX*-T_{AgTEF1}-loxP-T_{ADH1}-*ERG10*-P_{GAL10}-P_{GAL1}-*ERG13*-T_{CYC1}	This study
CENses1C	CEN1, but *KanMX* cured	This study
CENses2	CENses1C**,** *ura3-52::*loxP-P_{KlURA3}-*KlURA3*-T_{KlURA3}-loxP-T_{ADH1}-*ERG19*-P_{GAL10}-P_{GAL1}-*IDI*-T_{CYC1}	This study
CENses3	CENses2, *leu2-3,112::*loxP-P_{AgTEF1}-*SpHIS5*-T_{AgTEF1}-loxP-T_{ADH1}-*ERG12*-P_{GAL10}-P_{GAL1}-*ERG8*-T_{CYC1}	This study
CENses4	CENses3, *his3Δ1::* loxP-P_{KlLEU2}-*KlLEU2*-T_{KlLEU2}-loxP-T_{ADH1}-*ERG20*-P_{GAL10}-P_{GAL1}-*tHMG1*-T_{CYC1}	This study
CENses5	CENses4, *erg9*::loxP-P_{AgTEF1}-*kanMX*-T_{AgTEF1}-loxP-P_{CTR3}-*ERG9*	This study
CENses5C	CENses5, but *KlURA3*, *SpHIS5*, *KlLEU2*, *kanMX* cured	This study
CENses5C(+D)	CENses5C, expressing pYES2-*ScaGerD(+)*	This study
CENses5C(−D)	CENses5C, expressing pYES2-*ScaGerD(−)*	This study
CENses6(+D)	CENses5C, *gal80::*loxP-P_{KlLEU2}-*KlLEU2*-T_{KlLEU2}-loxP-P_{ADH1}-*ScaGerD(+)*-T_{PGK1}	This study
CENses6(−D)	CENses5C, *gal80::*loxP-P_{KlLEU2}-*KlLEU2*-T_{KlLEU2}-loxP-P_{ADH1}-*ScaGerD(−)*-T_{PGK1}	This study
CENses7(+D)	CENses6(+D), *lpp1::*loxP-P_{AgTEF1}-*SpHIS5*-T_{AgTEF1}-loxP-P_{ADH1}-*ScaGerD(+)*-T_{PGK1}	This study
CENses7(−D)	CENses6(-D), *lpp1::*loxP-P_{AgTEF1}-*SpHIS5*-T_{AgTEF1}-loxP-P_{ADH1}-*ScaGerD(−)*-T_{PGK1}	This study
CENses8(+D)	CENses7(+D), *rDNA::*loxP-P_{KlURA3}-*KlURA3*-T_{KlURA3}-loxP-P_{ADH1}-*ScaGerD(+)*-T_{PGK1}	This study
CENses8(−D)	CENses7(-D), *rDNA::*loxP-P_{KlURA3}-*KlURA3*-T_{KlURA3}-loxP-P_{ADH1}-*ScaGerD(−)*-T_{PGK1}	This study
CENses8(+D)*	CENses8(+D), expressing *pESC-YlACL1-2*	This study
CENses8(−D)*	CENses8(−D), expressing *pESC-YlACL1-2*	This study

synthetic complete (SC) medium or yeast extract, peptone, dextrose (YPD) medium at 30 °C with 200 rpm. YPD medium supplemented with G418 (200 μg/ml) was used for the selection of yeast strains carrying *kanMX* marker. Synthetic-defined (SD) medium (SC medium containing glucose) without uracil/leucine/histidine/tryptophan was chosen for auxotrophy selection of yeast strains. Culture stock containing 20% glycerol was prepared and stored at − 80 °C for long-term.

Preparation of plasmid constructs

Genomic DNA of CEN.PK2.1C (thereafter designated as CEN0) was used as template to PCR amplify the coding sequences of yeast ERG genes (*ERG8*, *ERG10*, *ERG12*, *ERG13*, *ERG19*, *ERG20*, *tHMG1*, and *IDI*) using Phusion High-Fidelity DNA Polymerase (https://www.thermofisher.com) and oligonucleotide primers (Table S1) and cloned into yeast episomal plasmid pESC. To prepare

pESC-*ERG10-ERG13* plasmid, *ERG10* (1194 bp) and *ERG13* (1473 bp) coding sequences were inserted into pESC-HIS using *Not*I/*Spe*I and *Bam*HI/*Sal*I restriction enzymes. To prepare pESC-*ERG19-IDI* plasmid, *ERG19* (1188 bp) and *IDI* (864 bp) coding sequences were inserted into vector pESC-URA using *Eco*RI/*Spe*I and *Bam*HI/*Sal*I. To prepare pESC-*ERG12-ERG8* plasmid, *ERG12* (1329 bp), and *ERG8* (1353 bp) coding sequences were inserted at the *Not*I/*Spe*I and *Bam*HI/*Sal*I restriction sites in pESC-LEU. To prepare pESC-*ERG20-tHMG1*, *ERG20* (1056 bp), and *tHMG1* (1575 bp, encoding 525 amino acids of C-terminal of *S. cerevisiae* HMG1) coding sequences were cloned at the *Not*I/*Spe*I and *Bam*HI/*Sal*I sites in pESC-LEU. pYES2-*ScaGerD(+)* and pYES2-*ScaGerD(−)* were prepared by inserting the codon-optimized *ScaGerD(+)* and *ScaGerD(−)* (1656 bp) into *Eco*RI/*Xho*I site of pYES2/NTB. pESC-*YlACL1-2* was prepared by inserting codon-optimized *YlACL1* (1950 bp) and *YlACL2* (1491 bp) into *Bam*HI/*Sal*I and *Not*I/*Spe*I site of pESC-TRP. Codon-optimized *ScaGerD(+)*, *ScaGerD(−)*, *YlACL1*, and *YlACL2* were designed and synthesized (synthesized genes were purchased from M/s Link Biotech, New Delhi and M/s Biotech Desk, Hyderabad). The integrity of cloned inserts was verified by restriction digestion and insert sequencing.

Yeast transformation

To prepare yeast competent cells, primary culture was prepared in YPD medium and incubated at 30 °C with 200 rpm for 16–18 h. The number of cells required to attain $OD_{600\,nm}$ of 0.4 was used to prepare a fresh culture in 50 ml YPD media and incubated at 30 °C for 3 h with 200 rpm. Cells were collected by centrifugation at 1500 × g for 10 min and washed in 40 ml 1 × TE (10 mM Tris, pH7.5, and 1 mM EDTA) and subsequently with 5 ml buffer A (100 mM lithium acetate, pH7.5, and 0.5 × TE). Finally, yeast cells were resuspended in 1 ml buffer A and incubated for 10 min. For yeast transformation, 125 µl of yeast competent cells were mixed with 1–1.5 µg plasmid (or PCR product), 12.5 µl ssDNA (10 mg/ml), and 875 µl buffer B (100 mM lithium acetate, pH7.5, and 1 × TE and 40% PEG-3350) in a 1.5-ml-microcentrifuge tube and incubated at 30 °C for 30 min with intermittent mixing at 10-min interval. Filter-sterilized DMSO was added, mixed by inverting, and the tube was placed in a water bath at 42 °C for 7 min. Furthermore, the tube was centrifuged for 10 s, and the supernatant was discarded. The cell pellet was washed with 1 × TE, resuspended in YPD medium and incubated for 3 h at 30 °C with 200 rpm before plating them, using appropriate selection medium (SD without uracil/leucine/histidine/tryptophan or YPD with G418).

Genomic DNA isolation and PCR confirmation of transformed strains

Yeast culture was prepared in YPD broth for 14–16 h at 30 °C with 200 rpm. The cells were harvested by centrifugation at 1500 × g for 1 min. The cell pellet was resuspended in lysis buffer (10 mM Tris-HCl pH8, 2% triton-X 100, 1% SDS, 100 mM NaCl, and 1 mM EDTA) and subjected to a freeze-thaw cycle three times (3–5 min freeze in liquid N_2 and 1 min in boiling water). An equal volume of Tris saturated phenol pH8 and chloroform was added and mixed for 2 min and centrifuged at 13,000 × g for 7 min to separate aqueous and organic phases. The upper aqueous layer was aliquoted into a fresh microcentrifuge tube, and genomic DNA (gDNA) was precipitated by mixing with 1/10th volume of 3 M sodium acetate (pH5.2) and 2.5 volumes of 99% ethanol (ice cold), and incubating at − 20 °C for 30 min. DNA precipitate was collected by centrifugation at 13,000 × g for 10 min at 4 °C. The pellet was washed with 70% ethanol (ice cold), air-dried, and dissolved in MilliQ water. gDNA was treated with RNase A and purified using polyethylene glycol. The gDNA isolated from transformed yeast colonies was used to confirm site-specific integration of DNA into yeast genome using locus-specific primers (Table S1).

Generation of yeast strains

For preparing genomic integration cassettes, the flanking sequences of the targeted genomic loci (*LYS5*, *ura3*, *leu2*, *his3*, *ERG9*, *GAL80*, *LPP1*, and *rDNA*), loxP-marker cassettes (*kanMX*, *KlURA3*, *SpHIS5*, and *KlLEU2*) and expression cassettes for ERG genes (*ERG10*, *ERG13*, *tHMG1*, *ERG12*, *ERG8*, *ERG19*, *IDI*, and *ERG20*), germacrene D synthases [*ScaGerD*(+), *ScaGerD(−)*] or P_{CTR3} promoter were PCR amplified using CEN0 genomic DNA, marker plasmids (pUG6, pUG27, pUG72, and pUG73) and pESC/pYES2 clones as templates (Table 1; primer sequences listed in Table S1). The individual PCR products were agarose gel purified, mixed in equimolar ratio, and transformed into CEN0 or derived strains following the lithium acetate transformation method as described above to integrate expression cassette at targeted locus and generating CENses1–8 strains (Table 1). The transformed colonies were selected on YPD medium containing G418 (200 µg/ml) or SD medium without uracil/histidine/leucine. The oligonucleotide primers contained ~ 30 bp overlapping sequences between adjacent fragments, which facilitated DNA assembly in the order: flanking sequence target locus-loxP-marker-loxP-*ERG* gene or *ScaGerD* expression cassette or P_{CTR3} promoter-flanking sequence target locus. The integration of

expression cassette/P_{CTR3} promoter into the genome at the target locus was confirmed by PCR analysis using locus-specific primers (Table S1).

In order to reuse the marker cassette for subsequent yeast transformation, the marker was rescued from the transformed strains following the Cre-LoxP system (Gueldener et al. 2002). The Cre-recombinase encoding plasmid, pSH63 was transformed into yeast strain following the lithium acetate transformation method and the transformed colonies were grown for 16 h in YPD medium supplemented with 2% (w/v) galactose to induce the expression of Cre-recombinase driven by galactose-inducible P_{GAL1} promoter. From the galactose-grown culture, about 250–300 colonies were selected in YPD medium and 40–50 colonies were tested for G418 sensitivity or uracil/histidine/leucine auxotrophy depending on the marker cassette. To further confirm whether the marker cassette was correctly excised from the strains, the genomic DNAs of selected colonies were tested in PCR using loci-specific primers. CENses8(+D)* and CENses8(−D)* strains were generated by transforming CENses8(+D) and CENses8(−D) with pESC-*YlACL1-2* plasmid. The detailed methods for the generation of yeast strains are presented in SI Methods.

Yeast culture and metabolite extraction

For the expression of galactose inducible genes in yeast, primary culture was prepared in SD medium (5 ml) and incubated at 30 °C with 200 rpm for 24 h. Secondary culture (20 ml) was prepared in 250-ml narrow-mouth unbaffled Erlenmeyer flask using freshly prepared SD medium by adding 0.1% (v/v) of primary culture and cultivated for 14–16 h at 30 °C with 200 rpm. The number of cells required to attain $OD_{600\ nm}$ of 0.6–1.0 was resuspended in freshly prepared SC medium (20 ml) containing 2% galactose, 1% raffinose, and 200 µM $CuSO_4$ (SG medium containing raffinose and $CuSO_4$) and incubated at 30 °C with 200 rpm. After 6 h, n-dodecane (10% v/v) was added, and the culture was allowed to grow at 30 °C. For the constitutive production of germacrene D, yeast primary culture was prepared in SD medium (5 ml) and incubated at 30 °C with 200 rpm for 24 h. In the $OD_{600\ nm}$, the culture was determined, and the number of cells that required attaining $OD_{600\ nm}$ of 0.1 was added in SD medium (20 ml) containing 200 µM $CuSO_4$ and n-dodecane (10% v/v), and the culture was continued to grow at 30 °C with 200 rpm. At different time intervals, n-dodecane phase was collected (centrifugation at 1500 × g for 10 min) and analyzed in gas chromatography-flame ionization detector (GC-FID) and gas chromatography-mass spectrometry (GC-MS).

Fed-batch fermentation

Primary culture was prepared in SD medium (5 ml) using 7–10 freshly grown colonies of yeast strain (pre-grown in SD medium with appropriate selection for auxotrophy) and incubated at 30 °C with 200 rpm for 24 h. The $OD_{600\ nm}$ of the culture was determined and the number of cells required to attain $OD_{600\ nm}$ of 0.15–0.2 was added in 250-ml narrow-mouth unbaffled Erlenmeyer flask containing SD medium (20 ml) with glucose as the carbon source and incubated at 30 °C until the $OD_{600\ nm}$ reached 0.5. After that, n-dodecane (10% v/v) and 200 µM $CuSO_4$ were added to the culture and incubated at 30 °C with continuous shaking at 200 rpm. At every 24-h intervals, the culture was supplemented with a carbon source (glucose, galactose, ethanol, glycerol, or pyruvate) at a final concentration of 2%, yeast extract (0.17%), and 200 µM $CuSO_4$ to compare the effect of different carbon sources on the production of germacrene D in fed-batch fermentation. The pH of the culture was adjusted to pH5.8 using 30% NaOH. The culture was harvested at 24-h intervals; n-dodecane phase was collected by centrifugation at 1500 × g for 10 min and analyzed by GC-FID. The concentration of glucose in yeast culture was estimated following the DNS (3,5-dinitro salicylic acid) method, as described previously with few modifications (Sengupta et al. 2000). Briefly, 150 µl DNS reagent (1% DNS, 20% sodium potassium tartrate and 2% of 2 M NaOH) was mixed with 150 µl of culture supernatant and placed in a boiling water bath for 5 min. Furthermore, the samples were cooled with running water and diluted with 700 µl of MilliQ water before taking absorbance (540 nm) in a UV-Vis spectrophotometer. A standard curve of glucose was considered for the quantification. Dissolved oxygen (DO) in yeast culture was estimated using a 235-mm-DO probe (Getinge-Applikon).

GC-FID and GC–MS analyses

An Agilent 7890B fitted with an Elite-5 column (30 m × 0.25 mm × 0.25 µm) was used to analyze metabolite in GC-FID. H_2 gas was the mobile phase (flow rate: 1 ml/min). The GC column oven temperature was programmed from 60 to 240 °C at a rate of 5 °C/min, with a final hold time of 4 min and total run time of 40 min. The oven temperature was maintained at 320 °C for 1 min before the GC run was completed. During the run, the split and split less injectors and flame ionization detector (FID) were kept at 300 °C with a split ratio of 10:1 (flow rate:10 ml/min). The identification of metabolite was done based on the retention time in GC-FID in comparison with authentic standards germacrene D (Cayman Chemical, USA), nerolidol and farnesol (Sigma-Aldrich, USA). Standard curves of germacrene D, nerolidol and farnesol were prepared for quantitative analysis of metabolites in GC-FID. Germacrene

D enantiomers were analyzed in chiral GC (Chanotiya and Yadav 2008). For GC-MS analysis, a PerkinElmer Clarus 680 GC system outfitted with a PerkinElmer Elite 5MS column (30 m × 0.25 mm × 0.25 µm) coupled with a PerkinElmer Clarus SQ 8C mass spectrometer was used. A programmed auto sampler-equipped injector injected about 1 µl of sample into a split injection mode 10:1. Helium gas (flow rate: 1.0 ml/min) was used as the carrier gas. Column oven temperature was set to ramp from 60 to 240 °C at a rate of 5 °C/min with a final hold time of 4 min with a run time of 40 min. The ion source and injector temperatures were 200 and 250 °C, respectively. The identification of metabolites was based on EI-MS spectra and retention time with comparison to authentic standards. Full mass spectra were recorded for metabolite identification by scanning across the *m*/*z* range of 50–600 amu with ionization mode EI+ at 70 eV. The scan time and inter-scan delay were set to 0.8 s and 0.01 s, respectively. For identification purpose, selected ion recording (SIR) for masses (*m*/*z* 183, 204) was also done with 0.2 s dwell time.

qRT-PCR analysis

Yeast cell pellet was obtained by centrifugation (1500 × g at 4 °C) and washed with ice-cold DEPC-treated MilliQ water. RNA was isolated using RNAiso Plus as per manufacturer's instructions (DSS Takara Bio India Pvt. Ltd.) with few modifications. Cell pellet was resuspended in RNAiso Plus and cell disruption was done using acid-washed glass beads (425–600 µm) at 4 °C by following three-cycles of 1 min vigorous vortexing. The integrity and quality of the RNA was confirmed by analyzing the $A_{260/280}$ and $A_{260/230}$ ratios using a Nanodrop spectrophotometer (NanoDrop One^{C}) and resolving on 1.2% denaturing (w/v) agarose gel. cDNA was synthesized using High-Capacity cDNA reverse transcriptase kit (Thermo Fisher Scientific). qRT-PCR was performed using SYBR Premix Ex Taq (Tli RNase H Plus) (DSS Takara Bio India Pvt. Ltd.) in a QuantStudio™ 5 system (Applied Biosystems, Thermo Fisher Scientific). The relative gene expression was calculated following the $2^{-\Delta\Delta ct}$ method using *ACT1* as an endogenous control, as described previously (Kumar et al. 2021). *ScaGerD(−)* and *ScaGerD(+)* copy numbers in engineered strains were determined in qRT-PCR, as described previously with few modifications (Shi et al. 2014). *ACT1*, a single copy gene in *S. cerevisiae* was used as a reference gene. To prepare standard curves and estimate PCR efficiency (E) of *ScaGerD(−)*, *ScaGerD(+)*, and *ACT1*, tenfold serial dilutions of pYES-*ScaGerD(−)*, pYES- *ScaGerD(+),*and pGEMT-*ACT1* plasmids and *S. cerevisiae* genomic DNA were prepared and used as templates in qRT-PCR analysis using SYBR Premix Ex Taq (Tli RNase H Plus). *ScaGerD(−)* and *ScaGerD(+)* copy numbers in engineered strains were estimated with reference to the standard curves and normalized with the copy number of *ACT1*.

Protein isolation and western blot analysis

Primary culture was prepared in 5 ml SD medium and incubated at 30 °C with continuous shaking for 24 h. Primary culture (0.1% (v/v) was used for secondary inoculation in 25 ml SD medium. From this, the culture volume that required attaining $OD_{600\ nm}$ 0.6 was resuspended in fresh 50 ml induction media with 2% galactose, 1% raffinose and 200 µm $CuSO_4$ and incubated at 30 °C with continuous shaking at 200 rpm for 16 h. Cells were collected by centrifugation (1500 × g for 4 min at 4 °C), and protein was extracted by the TCA method, as described in Yeast Protocols Handbook (Clontech). The protein was assessed using 10% SDS-PAGE and then proceeded for Western blot analysis. Towbin's buffer (25 mM Tris, 192 mM glycine, 20% methanol, and 0.01% SDS) was used to transfer the protein (100 µg) to the Amersham Hybond™-P PVDF Transfer Membrane (Pore size: 0.45 µm). Blocking was carried out for 2 h at room temperature using 5% skimmed milk in 1 × TBST buffer, which is composed of 1 × TBS (20 mM Tris pH7.5, 150 mM NaCl) and 0.1% Tween 20. The blot was washed with 1 × TBST 3–5 times before being incubated with the primary antibody (rabbit anti-His antibody, 1:7500 dilution, GenScript) overnight at 4 °C with shaking. After washing, the blot was incubated for 2 h at room temperature with a secondary antibody (goat anti-rabbit IgG (H&L)-HRP pAb, 1:10,000 dilution, GenScript). The blot was then developed using a Lumisensor Chemiluminescent HRP substrate (GenScript) and imagined using a Chemi Doc imager (Omega Lum C).

Results

Engineering ERG pathway to develop a chassis yeast strain

First of all, it was aimed to engineer an *S. cerevisiae* chassis strain that will produce FPP, the germacrene D precursor at a high level. To this end, the genes of the pre-FPP stage of the ERG pathway were overexpressed in *S. cerevisiae* (Fig. 1). Although the rate-limiting function of some of the ERG enzymes such as HMG1/2 was known, the regulation of individual enzymes towards ERG pathway activity remained to be clearly understood (Jordá and Puig 2020). Therefore, all the eight ERG pathway genes (*ERG10*, *ERG13*, *tHMG1*, *ERG12*, *ERG8*, *ERG19*, *IDI*, and *ERG20*) were considered for overexpression in CEN0 (Fig. 1). Moreover, post-FPP step of the ERG pathway was repressed to restrict FPP utilization for ergosterol biosynthesis, so that FPP flux would be

efficiently diverted towards germacrene D. For this purpose, endogenous promoter of the *ERG9* was chosen for replacement with P_{CTR3} for copper-mediated repression of the post-FPP step of the ERG pathway.

With the overall goal to increase FPP supply towards germacrene D biosynthesis, the strain CENses1 was developed by genomic integration of *ERG10–ERG13* expression cassette at the *lys5* locus of CEN0 strain (Fig. 2A). Subsequently, CENses2, CENses3, and CENses4 strains were generated following the integrations of *ERG19-IDI*, *ERG12-ERG8*, and *ERG20-tHMG1* expression cassettes at *ura3*, *leu2*, and *his3* loci of CENses1, CENses2, and CENses3, respectively (Table 1). All the target ERG pathway genes were expressed under the control of the bi-directional P_{GAL1}/

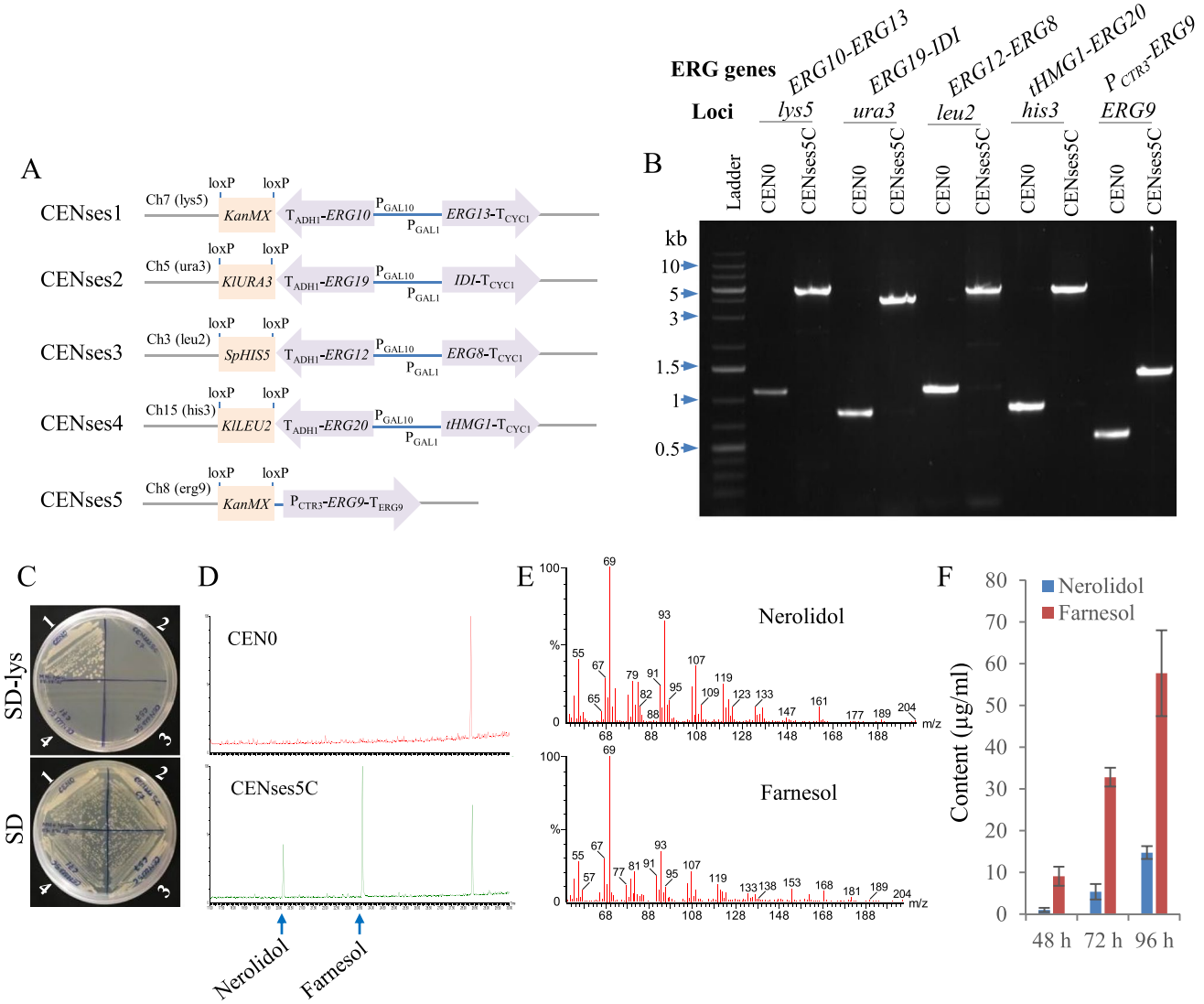

Fig. 2 CENses5C produced FPP-derived metabolites. **A** Schematic representation of genomic organization at *lys5*, *ura3*, *leu2*, *his3*, and *ERG9* loci in engineered strains CENses1–5. CENses1–4 strains were developed by integrating ERG gene expression cassettes (*ERG10-ERG13*, *ERG19-IDI*, *ERG12-ERG8*, and *tHMG1-ERG20*) in the *lys5*, *ura3*, *leu2*, and *his3* loci of CEN0 (CEN.PK2.1C) to CENses3. CENses5 was developed by replacing native promoter of *ERG9* with a copper-repressible P_{CTR3} promoter. **B** PCR fingerprinting of CEN0 and CENses5C (marker rescued version of CENses5) showing integrity of genomic modifications at the five targeted loci. PCR was carried out using locus-specific primers, and PCR products were resolved in 0.8% agarose gel. **C** Growth analysis of CEN0 and CENses5C strains in SD medium (without lysine) confirmed lysine auxotrophy of CENses5C. 1, CEN0 colony; 2–4, CENses5C colonies. **D** CENses5C produced FPP-derived metabolites nerolidol and farnesol when cultured in SC medium supplemented with 2% galactose, 1% raffinose, and 200 μM $CuSO_4$. GC-MS chromatogram detecting nerolidol and farnesol in CENses5C but not in CEN0. **E** The identity of nerolidol and farnesol produced in CENses5C was confirmed through verification of electron impact-mass spectrum (EI-MS) patterns in GC-MS analysis. **F** The amount of nerolidol and farnesol produced in CENses5C was determined in GC-FID analysis using reference standard curves for nerolidol and farnesol. Data are *mean* ± *SE*, $n = 3$ independent cultures

P_{GAL10} promoter of *S. cerevisiae* (Fig. 2A). Considering the negative feedback regulation of HMG1, *tHMG1* encoding the C-terminal catalytic domain (525 amino acids) of native HMG1 was overexpressed instead of the full-length protein. In the next step, the native promoter of *ERG9* in CENses4 strain was replaced with the copper-repressible promoter P_{CTR3} to produce CENses5 (Fig. 2A). It was known that the P_{CTR3} promoter is repressed in the presence of copper, but it remains activated in copper-deprived conditions. P_{CTR3} promoter bears two cis-acting copper-responsive elements (TTT GCTC) that restrict the expression of *S. cerevisiae CTR3* gene in the availability of $CuSO_4$ (Labbé et al. 1997). To this end, a 734-bp P_{CTR3} promoter was integrated immediate upstream of the translation start codon (ATG) of *ERG9*. The integrity of all five engineered loci in CENses5C (a marker rescued derivative of CENses5) that was created with the aim to overexpress eight ERG pathway enzymes and downregulate *ERG9* was verified through PCR using locus-specific primers (Table S1; Fig. 2B). Due to the disruption of *LYS5* locus, CENses1, and subsequent strains became auxotrophs for lysine. This property of engineered yeast strains helped us to easily distinguish the engineered strains from the commonly grown laboratory strains of *S. cerevisiae* (Fig. 2C).

To test whether CENses5C can produce an increased level of FPP than CEN0, these strains were grown in SD medium until $OD_{600\ nm}$ of 0.6 and subsequently cultured for 48 h in SC medium supplemented with 2% galactose, 1% raffinose, and 200 µM $CuSO_4$ (SG medium containing raffinose and $CuSO_4$), and the culture was overlaid with 10% n-dodecane. It was known that the increased accumulation of FPP in *S. cerevisiae* leads to biosynthesis of two FPP-derived isomeric metabolites nerolidol and farnesol, possibly alleviating metabolic burden and toxic effect due to over-accumulation of FPP (Rodriguez et al. 2014). CENses5C showed a comparatively reduced growth rate than CEN0, which might be due to the accumulation of FPP at a toxic level in the absence of an efficient downstream pathway (Figure S1). Moreover, gas chromatography-mass spectrometry (GC-MS) analysis of metabolites sequestered in n-dodecane layer of CEN0 and CENses5C cultures detected nerolidol and farnesol in CENses5C, but not in CEN0 (Fig. 2D, E). Nerolidol and farnesol titers in CENses5C were 14.71 µg/ml and 57.71 µg/ml at 96 h of culture (Fig. 2F). These results suggested increased biosynthesis of FPP in CENses5C strain, which was subsequently converted to farnesol and its isomer nerolidol following dephosphorylation by endogenous yeast phosphatase(s). The FPP dephosphorylation in CENses5C might be due to the action of LPP1 and DPP1 enzymes, which were found to contribute to the most of isoprenoid phosphate phosphatase activity in yeast (Faulkner et al. 1999). Moreover, qRT-PCR analysis of the transcript levels of ERG genes revealed galactose-induced expression of *ERG8*, *ERG10*, *ERG12*, *ERG13*, *ERG19*, *ERG20*, *IDI*, and *HMG1* in CENses5C (Fig. 3). However, *ERG9* showed copper-repressible expression in CENses5C. Overall, these results indicated higher FPP level in CENses5C strain due to the upregulation of the upstream ERG pathway and repression of *ERG9* that restricted FPP flux to the ergosterol (Fig. 1). Thus, CENses5C could be a favorable strain for high-level production of FPP-derived sesquiterpenes such as germacrene D by expressing sesqui-TPSs.

Overproduction of (+) and (−)-germacrene D in ERG pathway-engineered CENses5C

S. canadensis essential oil is a rich source of germacrene D and two germacrene D synthases (Sc11 and Sc19) that selectively produced (+) or (−)-germacrene D, were identified (Prosser et al. 2004; Chanotiya and Yadav 2008). Therefore, *Sc11* and *Sc19* were chosen as the best candidates for expression in CENses5C strain. To address the issue of translational efficiency of plant genes in yeast, *Sc11* and *Sc19* genes were codon optimized, considering codon usage bias of *S. cerevisiae* (https://www.kazusa.or.jp/codon/cgi-bin/showcodon.cgi?species=4932) and by removing cryptic splicing sites (GGTGAT in *Sc11* and *Sc19*), premature PolyA site (ATTAAA in *Sc19*), mRNA destabilizing sites (ATTTA in *Sc11* and *Sc19*), and repeat sequence (TCAAGAATATTC TTGA). The codon-optimized sequences were designated as *ScaGerD(+)* and *ScaGerD(−)* (Figure S2). GC content was adjusted from 38.6 to 33.6% for *ScaGerD(+)* and 38.9 to 36% for *ScaGerD(−)* by removing the peaks of % GC content in a 60-bp window. Codon Adaptation Index (CAI) was increased from 0.73 to 0.91 for *ScaGerD(+)* and 0.58 to 0.83 for *ScaGerD(−)*. *ScaGerD(+)* and *ScaGerD(−)* were expressed in CENses5C under the control of galactose-inducible P_{GAL1} promoter using pYES2/NTB episomal plasmid. These strains were designated as CENses5C(+D) and CENses5C(−D) (Table 1). The metabolites produced in CENses5C(+D) and CENses5C(−D) after galactose induction were sequestered in n-dodecane layer of yeast culture and analyzed following chiral GC-MS method (Fig. 4A). The analysis clearly detected (+) and (−)-germacrene D as major products in CENses5C(+D) and CENses5C(−D), respectively. The identity of (+) and (−)-germacrene D produced in CENses5C(+D) and CENses5C(−D) was verified with a comparison of retention time and EI-MS spectra of (+) and (−)-germacrene D found in the essential oil of *S. canadensis* (Fig. 4A, B). Moreover, quantitative GC-FID determination of (+) and (−)-germacrene D detected in CEN0 and CENses5C strains expressing *ScaGerD(+)* and *ScaGerD(−)* revealed significantly higher production of (+) and (−)-germacrene D in CENses5C(+D) and CENses5C(−D) than in CEN0(+D) and CEN0(−D) (Fig. 4C, D). CENses5C(+D) produced ~ 30-fold higher amount of (+)-germacrene D as

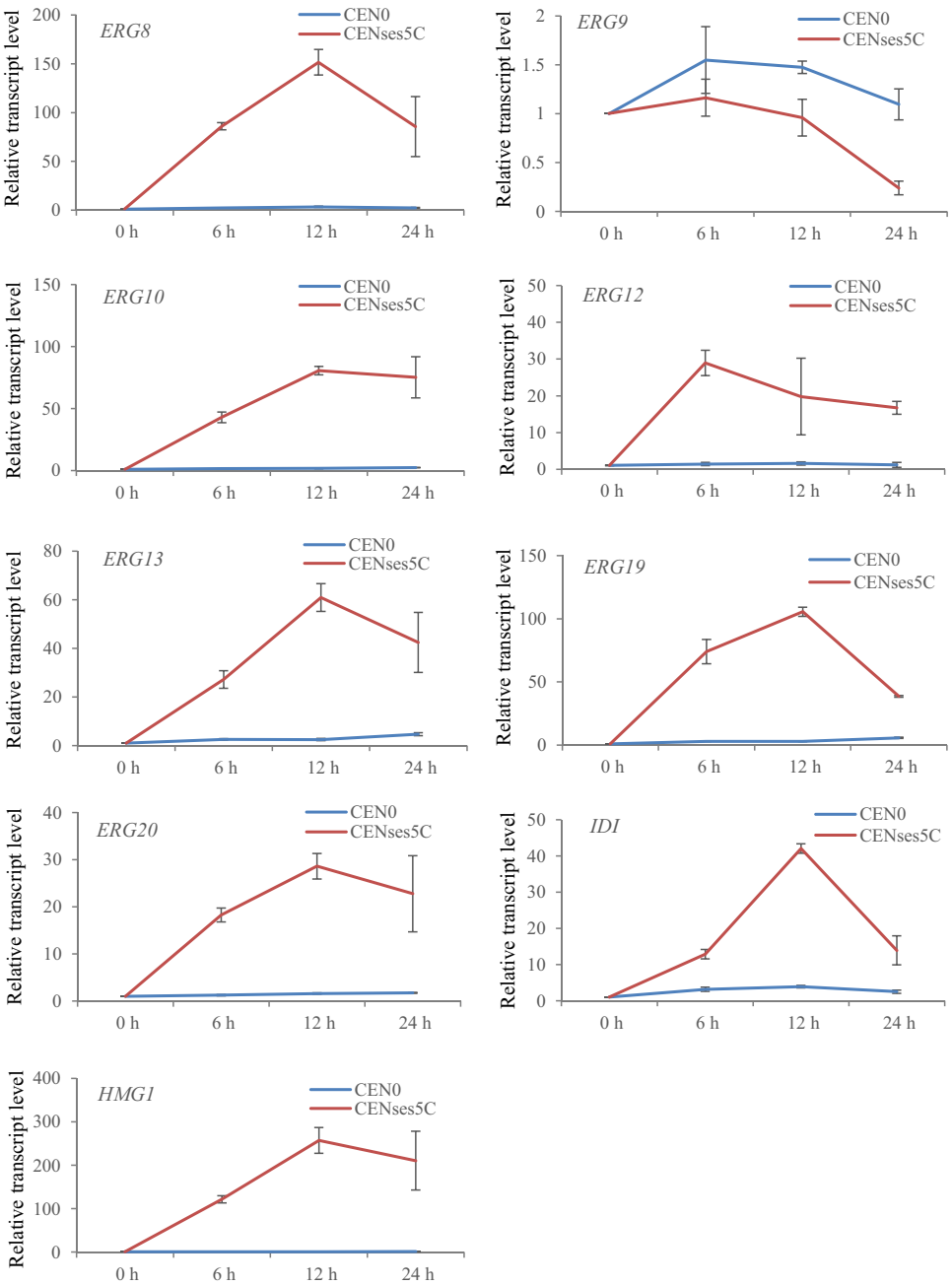

Fig. 3 Transcript expression of ERG pathway genes. qRT-PCR analysis of transcript level in CEN0 and CENses5C strains at different time intervals of culture in SC medium supplemented with 2% galactose, 1% raffinose, and 200 µM $CuSO_4$. Data are *mean* ± *SE*, $n = 3$ independent cultures

compared to CEN0(+D) in shake-flask culture at 144 h post-cultivation in SG medium supplemented with raffinose and $CuSO_4$. However, CENses5C(−D) produced ~ 13-fold higher amount of (−)-germacrene D as compared to CEN0(−D). Germacrene D produced in yeast strains was analyzed at different time intervals between 48 and 168 h post-cultivation in SG medium supplemented with raffinose and $CuSO_4$, but a higher amount of metabolites could be recovered at 144 h. The concentration of (+) and (−)-germacrene D in CENses5C(+D) and CENses5C(−D) cultures were 34.77 and 158.06 µg/ml at 144-h post-cultivation in SG medium supplemented with raffinose and $CuSO_4$ (Fig. 4D). Taken together, these results indicated overproduction of enantiopure germacrene D in engineered strain CENses5C as compared to CEN0.

Deletion of *GAL80* led to constitutive production of (+) and (−)-germacrene D in CENses6

The ERG genes, and *ScaGerD(+)* and *ScaGerD(−)* were expressed in CENses5C(+D) and CENses5C(−D) under the control of P_{GAL1}/P_{GAL10} promoter, which required galactose as an inducer of gene expression to produce (+) and (−)-germacrene D. However, a constitutive production platform of

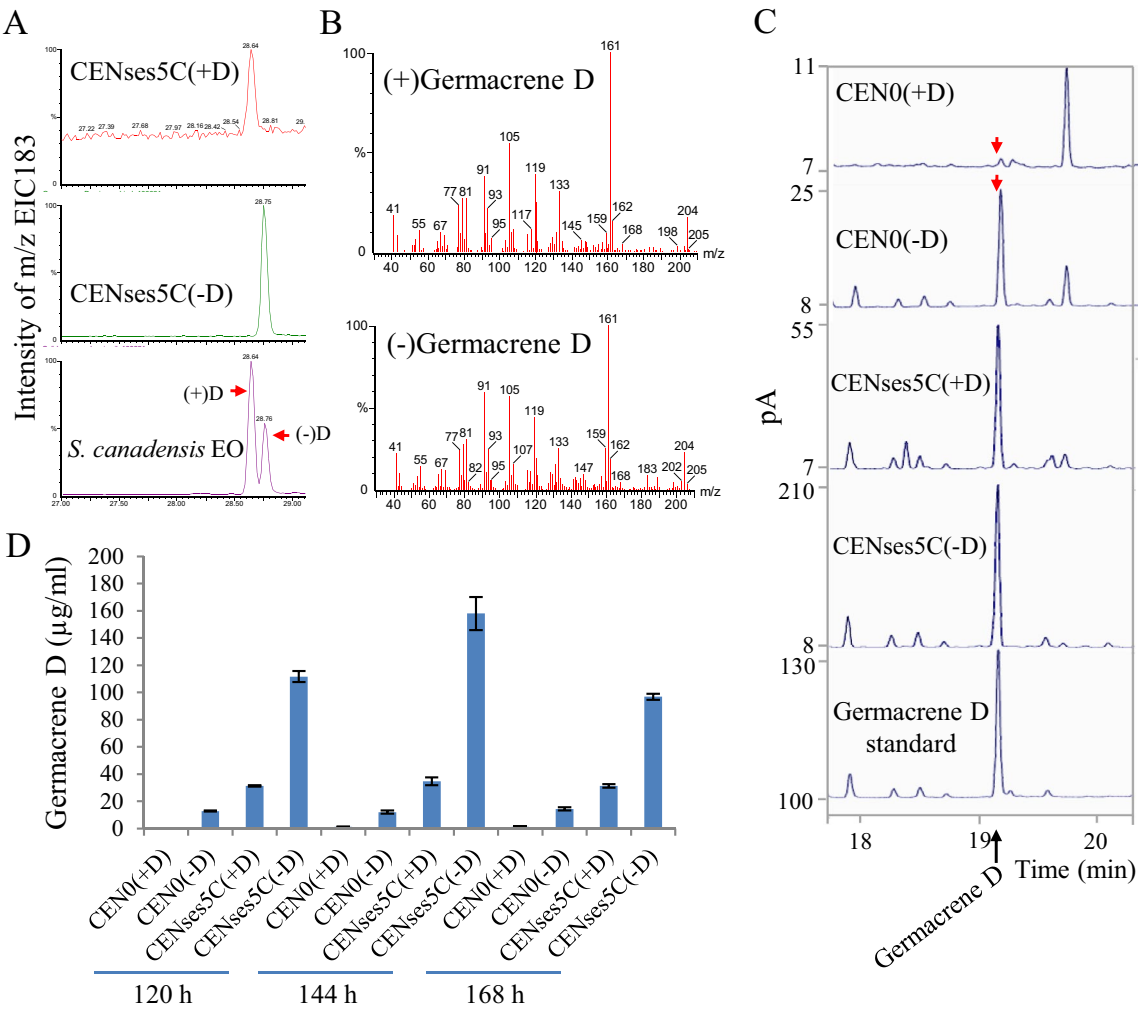

Fig. 4 CENses5C produced increased level of germacrene D. **A** Chiral GC-MS analysis detecting (+) or (−)-germacrene D in CENses5C, expressing either (+)-germacrene D synthase [*ScaGerD(+)*] or (−)-germacrene D synthase [*ScaGerD(−)*]. *S. canadensis* essential oil (EO) was used as reference. **B** EI-MS of germacrene D produced in CENses5C, which was similar to germacrene D detected in *S. canadensis* EO. **C** GC-FID analysis to quantify germacrene D titers in CEN0 and CENses5C expressing *ScaGerD(+)* or *ScaGerD(−)*. Yeast strains were initially cultured in SD medium until OD_{600nm} of 0.6 and subsequently grown for up to 168 h in SC medium with 2% galactose, 1% raffinose, and 200 µM $CuSO_4$. Representative GC-FID chromatograms of metabolites sequestered in n-dodecane in CEN0 and CENses5C cultures are shown. **D** A comparison of (+) and (−)-germacrene D titers in CEN0 and CENses5C expressing *ScaGerD(+)* or *ScaGerD(−)*. The amount of (+) and (−)-germacrene D was determined in GC-FID analysis using a reference standard curve of germacrene D. Data are *mean* ± *SE*, $n = 3$ independent cultures. (+D) and (−D) denote (+) and (−)-germacrene D, respectively

germacrene D without the requirement of an inducer of gene expression would help reduce input cost in large-scale industrial production. The disruption of *GAL80*, a negative regulator of GAL genes in *S. cerevisiae* was known to constitutively activate galactose-inducible promoters including P_{GAL1}/P_{GAL10} (Torchia et al. 1984). In order to achieve a constitute production platform of (+) and (−)-germacrene D, CENses6(+D) and CENses6(−D) strains were developed by disrupting *GAL80*. To this end, the expression cassettes of *ScaGerD(+)* and *ScaGerD(−)* were prepared using *S. cerevisiae* P_{ADH1} constitutive promoter and T_{PGK1} terminator, and the expression cassette was introduced into *GAL80* locus of CENses5C to develop CENses6(+D) and CENses6(−D) strains for the production of (+) and (−)-germacrene D, respectively (Table 1; Fig. 5A). qRT-PCR analysis confirmed single copy integration of *ScaGerD(+)* and *ScaGerD(−)* in CENses6(+D) and CENses6(−D) strains (Figure S3). The growth of CENses6(+D) and CENses6(−D) strains in SD (glucose) medium supplemented with 200 µM $CuSO_4$ led to constitutive production of germacrene D without the need for galactose and any terpene precursor supplementation in the medium (Fig. 5B). The amount of germacrene D produced in CENses6(+D) and CENses6(−D) strains was analyzed at different time intervals between 24

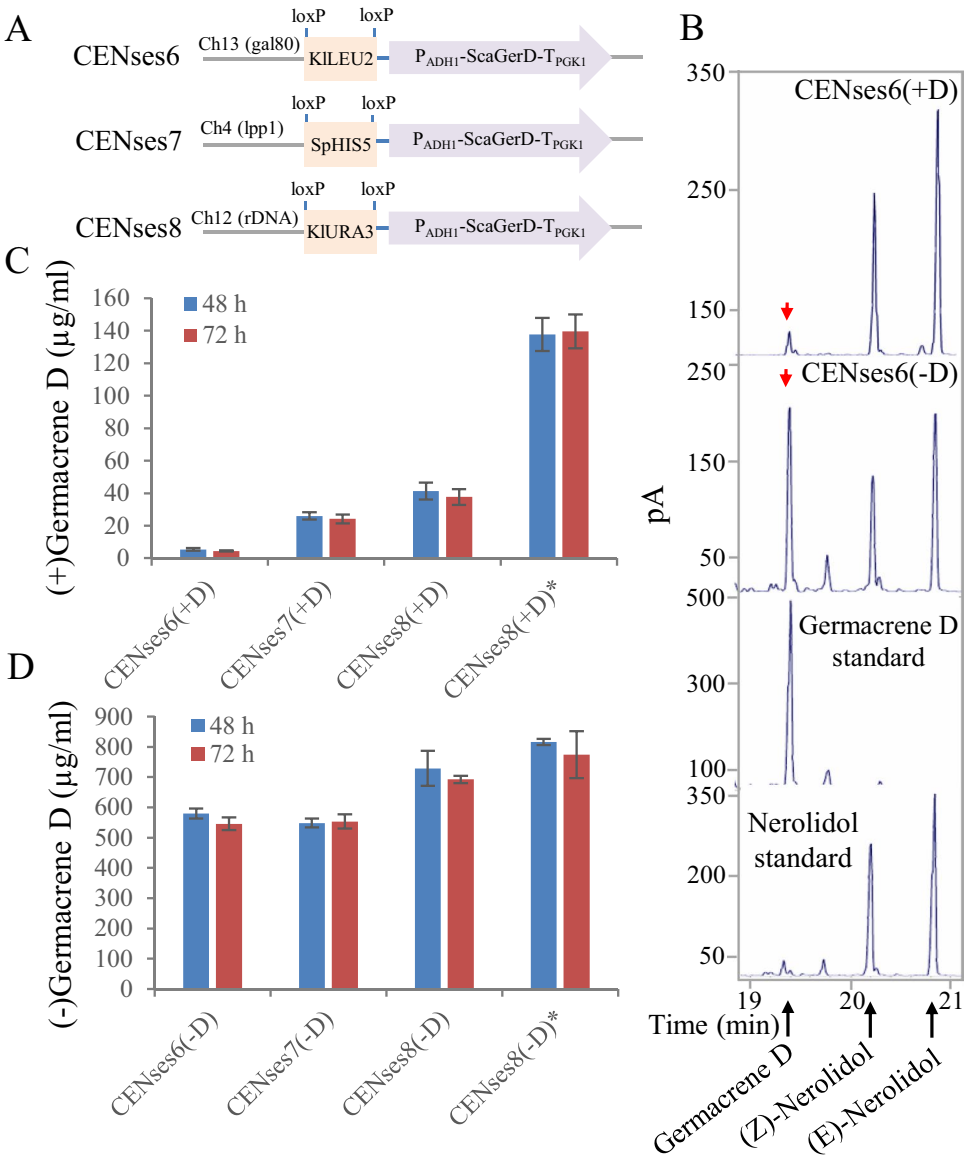

Fig. 5 Constitutive production of germacrene D in engineered strains. **A** Schematic representation of genomic organization at *gal80*, *lpp1* and rDNA loci in engineered strains CENses6–8 developed by integration of ScaGerD [*ScaGerD(+)* and *ScaGerD(−)*] expression cassettes. **B** GC-FID analysis quantified germacrene D titers in CENses6–8* strains using germacrene D reference standard. Nerolidol served as internal control. Strains were grown in SD medium supplemented with 200 µM $CuSO_4$. Representative GC-FID chromatograms of CENses6(−D) and CENses6(+D) strains are shown. **C** and **D** (+)-Germacrene D and (−)-germacrene D titers in the cultures of CENses6–CENses8* strains were estimated in GC-FID analysis using a standard curve of germacrene D. Data are *mean* ± *SE*, $n = 3$ independent cultures. (+D) and (−D) denote (+) and (−)-germacrene D, respectively

and 96 h after the addition of $CuSO_4$, but the highest titer could be achieved at 48 h. CENses6(+D) and CENses6(−D) produced 5.39 and 579.59 µg/ml (+) and (−)-germacrene D at 48 h after addition of $CuSO_4$, respectively (Fig. 5C, D). Notably, CENses6(+D) and CENses6(−D) displayed a similar growth rate as CENses5C(+D) and CENses5C(−D), suggesting that constitutive production of germacrene D did not affect yeast growth (Figure S4). Interestingly, (−)-germacrene D detected in CENses6(−D) was about 3.6-fold higher than CENses5C(−D) (Figs. 4D and 5D). Moreover, the amount of (−)-germacrene D estimated in the constitutive production platform of CENses6(−D) expressing *ScaGerD(−)* was about 100-fold higher than (+)-germacrene D found in CENses6(+D), which expressed *ScaGerD(+)*. Likewise, CENses5C(−D) strain transformed with pYES2-*ScaGerD(−)* plasmid also produced significantly higher amount of (−)-germacrene D than the amount of (+)-germacrene D detected in CENses5C(+D) strain harbouring pYES2-*ScaGerD(+)* plasmid (Table 1; Fig. 4D). However, ScaGerD(+) and ScaGerD(−) protein levels in the engineered strains were detected at comparable levels (Figure S5). Although the amount of (+) and (−)-germacrene D in *S. canadensis* essential oils might vary between cultivars, they were generally found in equal ratios or excess of (+)-germacrene D (Chanotiya and Yadav 2008). These results suggested that (−)-germacrene D synthase encoded by *ScaGerD(−)* worked more efficiently in yeast than (+)-germacrene D synthase encoded by *ScaGerD(+)*, which might be due to the different catalytic activity of these enzymes when expressed in plant and yeast hosts (Prosser et al. 2004). This difference in enzyme catalytic activity in plant and yeast hosts might be due to the difference in host microenvironment,

cofactor availability, and potential post-translational modifications. Overall, these results suggested constitutive production of (+) and (−)-germacrene D in CENses6(+D) and CENses6(−D) strains, respectively, without the need for galactose supplementation in culture media.

Improving (+) and (−)-germacrene D titers by disruption of *LPP1* gene and integrating multiple copies of germacrene D synthases in *rDNA* locus

LPP1 is one of the endogenous phosphatases in *S. cerevisiae* that might compete with ScaGerD(+) and ScaGerD(−) for FPP in the engineered yeast strains (Faulkner et al. 1999). In order to test whether disruption of *LPP1* can lead to higher production of germacrene D, an additional copy of P_{ADH1}-*ScaGerD*-T_{PGK1} expression cassette was introduced into the *LPP1* locus of CENses6(+D) and CENses6(−D), generating CENses7(+D) and CENses7(−D) strains (Table 1; Fig. 5A). qRT-PCR analysis using genomic DNAs of CENses7(+D) and CENses7(−D) strains confirmed two copies of *ScaGerD(+)* and *ScaGerD(−)* in the strains (Fig. 3). GC-FID analysis of n-dodecane-sequestered metabolites obtained from the cultures of CENses7(+D) grown in SD medium (supplemented with $CuSO_4$) revealed 4.81-fold increased titer of (+)-germacrene D in CENses7(+D) as compared to CENses6(+D) at 48 h post-$CuSO_4$ supplementation (Fig. 5C). (+)-Germacrene D titer in CENses7(+D) reached to 25.96 µg/ml. In contrast, (−)-germacrene D titer in CENses7(−D) remained unaltered when compared with CENses6(−D) strain, suggesting that LPP1 might not be competing with ScaGerD(−) in the engineered strains (Fig. 5D). The different outcomes of CENses7(+D) and CENses7(−D) strains for germacrene D titer could be due to the differential catalytic efficiency of ScaGerD(+) and ScaGerD(−) because their protein levels in the engineered strains were quite comparable (Figure S5). The better catalytic efficiency of ScaGerD(−) in yeast might led to a higher rate of conversion of FPP to germacrene D in the engineered strains, which might not allow accumulation of FPP in the cell. Furthermore, it will be interesting to examine how the deletion of *DPP1*, which was known to work redundantly with *LPP1*, might affect germacrene D titer in engineered yeasts (Faulkner et al. 1999).

We next tested whether integration of multiple copies of *ScaGerD(+)* or *ScaGerD(−)* in the engineered strains could result in further improvement in germacrene D titer. *S. cerevisiae* carries about 150 copies of 9.1 kb ribosomal DNA (*rDNA*) in tandem repeats on the right arm of the chromosome XII spanning an approximately 1–2 Mb region (Kobayashi et al. 1998). It was reported that multiple copies of foreign genes could be integrated into *rDNA* through homologous recombination, leading to enhanced production of terpenoids (Liu et al. 2018; Peng et al. 2022). To test this strategy of improved metabolite production, additional copies of P_{ADH1}-*ScaGerD*-T_{PGK1} expression cassette were integrated into *rDNA* locus of CENses7(+D) and CENses7(−D) strains to develop CENses8(+D) and CENses8(−D) strains (Table S1; Fig. 5A). qRT-PCR analysis of gene copy number revealed that CENses8(+D) and CENses8(−D) strains retained 4 copies of *ScaGerD(+)* and *ScaGerD(−)* in the genome (Figure S3). GC-FID analysis of (+) and (−)-germacrene D produced in engineered strains revealed 1.59 and 1.32-fold higher titers in CENses8(+D) and CENses8(−D) strains than in CENses7(+D) and CENses7(−D), respectively. (+) and (−)-Germacrene D titers in CENses8(+D) and CENses8(−D) were determined as 41.36 and 728.87 µg/ml at 48 h after supplementation with $CuSO_4$, respectively (Fig. 5C, D).

Expression of ATP citrate lyase increased germacrene D titer

ATP citrate lyase (ACL), which catalyzes the conversion of citrate, a TCA cycle intermediate to cytosolic acetyl-CoA in an ATP-dependent manner contributes to the high rate production of lipids in oleaginous yeast *Yarrowia lipolytica* (Fig. 1; Dulermo et al. 2015). However, ACL is absent in non-oleaginous yeast such as *S. cerevisiae*. The catalytically active ACL in *Y. lipolytica* is a heterodimer of the catalytic subunit ACL1 and a regulatory subunit ACL2. The expression of *ACL1* and *ACL2* was found to boost the titer of acetyl-CoA-derived metabolites in *S. cerevisiae* (Lian et al. 2014; van Rossum et al. 2016; Rodriguez et al. 2016). To test if ACL can further boost germacrene D titer by increasing acetyl-CoA pool in the cytosol, *Y. lipolytica ACL1*, and *ACL2* (*YlACL*) were expressed in CENses8(+D) and CENses8(−D) under the control of P_{GAL1}/P_{GAL10} promoter. To this end, *YlACL1* (YALI0E34793p) and *YlACL2* (YALI0D24431p) were codon-optimized, considering codon usage bias of *S. cerevisiae* (https://www.kazusa.or.jp/codon/cgi-bin/showcodon.cgi?species=4932), and by removing cryptic splicing sites (GGTAAG), mRNA destabilizing sites (ATTTA). GC content was adjusted from 55.8 to 36.8 for *YlACL1* and 61.8 to 37.5 for *YlACL2* by removing the peaks of % GC content in a 60-bp window. Codon Adaptation Index (CAI) was increased from 0.58 to 0.92 for *YlACL1* and 0.53 to 0.93 for *YlACL2*. The codon-optimized *YlACL1* and *YlACL2* were cloned into pESC episomal plasmid, generating pESC-*YlACL1-2* (Table 1 and Figure S6). CENses8(+D)* strain that expressed *YlACL1* and *YlACL2* from the pESC-*YlACL1-2* plasmid produced significantly higher titer of (+)-germacrene D than CENses8(+D) (Fig. 5C). GC-FID analysis revealed 137.71 µg/ml (+)-germacrene D in CENses8(+D)* at 48 h after supplementation with $CuSO_4$, which was 3.33-fold higher than the (+)-germacrene D titer estimated in CENses8(+D). However,

(−)-germacrene D titer (815.81 µg/ml) in pESC-*YlACL1-2*-transformed CENses8(−D)* was increased marginally (11.92%) over CENses8(−D) (Fig. 5D). This outcome on expressing *YlACL* in CENses8(−D)* might be due to the reason that (−)-germacrene D titer in CENses8(−D) already attained the maximum titer level that could be achieved in shake-flask fermentation. However, a more efficient ACL (e.g., ACL from *Aspergillus nidulans*) might be helpful in increasing acetyl-CoA pool and germacrene D titers in engineered strains (Rodriguez et al. 2016). Nevertheless, these results revealed a significantly increased titer of (+)-germacrene D in CENses8(+D)* following the expression of *YlACL*. Overall, (+)-germacrene D and (−)-germacrene D produced in CENses8(+D)* and CENses8(−D)* strains were 67–120 fold higher than their titers in CEN0 expressing pYES2-*ScaGerD(+)* or pYES2-*ScaGerD(−)*.

Fed-batch fermentation increased (+) and (−)-germacrene D titer

Fed-batch fermentation is frequently practiced to increase product titer in microbial fermentation (Ghiffary et al. 2022; Lin et al. 2022; Kim et al. 2022). To test if, (+) and (−)-germacrene D titers in CENses8 strains could be further improved, fed-batch fermentation was carried out using shake flasks. The strains were initially grown in SD media and supplemented with 200 µM $CuSO_4$ when $OD_{600\ nm}$ reached 0.5. Subsequently, yeast culture in SD medium was supplemented with 2% carbon source (glucose, galactose, glycerol, ethanol, or pyruvate), 0.17% yeast extract, and 200 µM $CuSO_4$ for every 24-h intervals after the first-time addition of $CuSO_4$, and the supplementation of carbon source, and $CuSO_4$ was continued for 24-h interval until 96 h. The metabolites sequestered in n-dodecane layer were collected from the culture at 48–120 h after first-time addition of $CuSO_4$ and analyzed in GC-FID. Among the carbon sources tested in fed-batch fermentation, 2% glucose fed produced higher yield of germacrene D in engineered strains (Fig. 6 and Figure S7). Under the fed-batch fermentation using glucose feed, (+)-germacrene D titer in CENses8(+D) strain was 201.37 µg/ml at 120 h (Fig. 6A). In CENses8(+D)* strain, (+)-germacrene D titer was further increased to 290.28 µg/ml, which was 1.44-fold improvement over CENses8(+D) (Fig. 6B). On the other hand, (−)-germacrene D titer in CENses8(−D) strain was 2379.18 µg/ml at 120 h under fed-batch fermentation (Fig. 6C). But, (−)-germacrene D titer (2519.46 µg/ml) in CENses8(−D)* strain showed a marginal increment (5.5%) over the titer in CENses8(−D) (Fig. 6D). Similar to (−)-germacrene D titer in batch fermentation in shake-flasks, CENses8(−D)* strain did not show significant improvement in (−)-germacrene D titer over CENses8(−D) strain under fed-batch

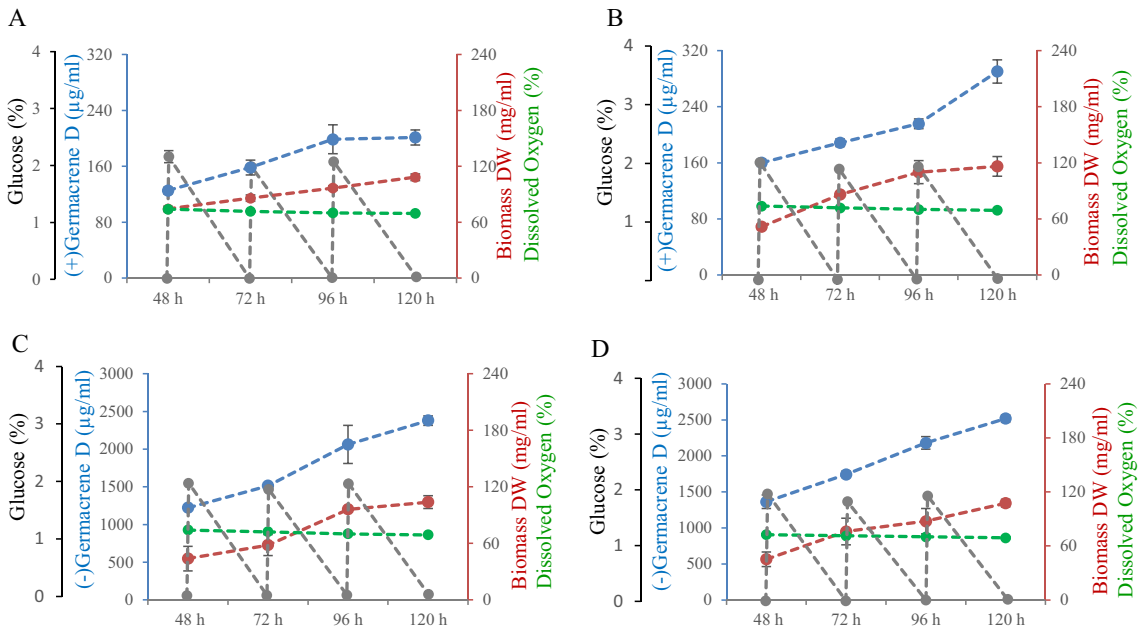

Fig. 6 Evaluation of CENses8 and CENses8* strains in fed-batch fermentation. **A**, **B**, **C**, and **D** The biomass and (+) or (−)-germacrene D yields in CENses8 and CENses8* strains. The strains were initially grown in SD media and supplemented with 200 µM $CuSO_4$ when $OD_{600\ nm}$ reached 0.5. Subsequently, the media was supplemented with 2% glucose, 0.17% yeast extract, and 200 µM $CuSO_4$ for every 24-h intervals, and germacrene D yield was estimated at different time intervals. Glucose and dissolved oxygen (DO) levels in the yeast culture are also plotted. Data are *mean* ± *SE*, $n = 3$ independent cultures. **A** CENses8(+D), **B** CENses8(+D)*, **C** CENses8(−D), and **E** CENses8(−D)*

fermentation in shake-flask (Fig. 5D). These results were unlike CENses8(+D)* strain, which showed better improvement in (+)-germacrene D titer over CENses8(+D) strain under the both batch and fed-batch culture in shake-flask (Figs. 5C and 6A, B). This discrepancy in responses of CENses8(+D)* and CENses8(−D)* strains could be due to the fact that the (−)-germacrene D titer in CENses8(−)D*, which was 8.68 fold higher than (+)-germacrene D titer in CENses8(+D)*, reached the maximum limit of production in shake-flask fermentation. Moreover, CENses8(−D) and CENses8(−D)* strains accumulated slightly less biomass than CENses8(+D) and CENses8(+D)* strains, suggesting that the higher metabolic flux to (−)-germacrene D in CENses8(−D) and CENses8(−D)* strains was compensated with cell biomass (Figure S8). Furthermore, studies of CENses8 strains in bioreactors might provide better insights into this aspect of germacrene D biosynthesis in engineered yeasts. Taken together, these results suggested increased titers of (+) and (−)-germacrene D under fed-batch fermentation in shake-flasks using 2% glucose feed.

Discussion

The tools of synthetic biology and metabolic engineering provide the opportunity for the production of industrially demanded fine chemicals in fast-growing microbial hosts to attain sustainable supply (Paddon and Keasling 2014; Srinivasan and Smolke 2020; Zhang et al. 2022; Ma et al. 2023). Metabolic engineering in *S. cerevisiae* to produce germacrene A was carried out in a couple of previous studies, which resulted in highest production titer of 309.8 mg/l in shake-flask batch culture (Hu et al. 2017; Bröker et al. 2020; Zhang et al. 2021). However, despite various applications of germacrene D in agricultural and fragrance industries, metabolic engineering for microbial production of germacrene D was not well explored, and germacrene D supply is still dependent on plant source, which has limitation for sustainable production and scalability of enantiopure products (Liu et al. 2022). The earlier study achieved 1.94 g/l (–)-germacrene D titer in shake-flask fermentation and 7.9 g/l (–)-germacrene D in a 5-l bioreactor in fed-batch fermentation by expressing *Acremonium chrysogenum AcTPS1* in *S. cerevisiae* (Liu et al. 2022). However, (+)-germacrene D yield in *S. cerevisiae* was about 775-fold less (2.5 mg/l) than (–)-germacrene D titer, and high-level production of (+)-germacrene D was not explored through yeast strain engineering. Furthermore, the germacrene D production platform relied on galactose as inducer of gene expression (Liu et al. 2022). On the other hand, (+) and (−)-germacrene D titers achieved in the present study using the engineered CENses8(+D)* and CENses8(−)D* strains are so far the highest reported titers of germacrene D enantiomers in shake-flask fermentation following a fed-batch process. The present work achieved ~ 29% increase in (−)-germacrene D and ~ 100 times increase in (+)-germacrene D titer as compared to previous work, considering germacrene D titers in shake-flask (Liu et al. 2022). The titers of germacrene D achieved in the present study were equivalent to 2.52 and 23.53 mg/g dry cell weight (DCW) for (+)-and (−)-germacrene D, respectively. Moreover, the present study for the first time implemented the strategy of overexpression of ACL of oleaginous yeast in ERG pathway-engineered *S. cerevisiae* to produce enantiopure germacrene D in microbial host. Moreover, the engineered yeast strains generated by disrupting *GAL80* gene led to a constitutive production platform of enantiopure germacrene D without the need for galactose-induced gene expression, which will help in reducing input costs in large-scale production platforms. Furthermore, it will be interesting to evaluate CENses8(+D)* and CENses8(−D)* strains in the large-scale bioreactor. The germacrene D titer in bioreactor is expected to be multiple folds higher than achieved in shake-flask fermentation considering previous work reported a 25 to 50-fold increase in terpenoid titers in bioreactor than in shake-flask (Paddon et al. 2013; Deng et al. 2022). In conclusion, this work presented a comprehensive metabolic engineering strategy in yeast involving eight genomic modification steps targeting multiple knock-outs (two genes) and over-expression (eight genes) of yeast genes, integration of multiple copies of expression cassettes of plant germacrene D synthases and coupling of TCA cycle intermediate to ERG pathway, leading to directed flux of terpenoid precursor for the high-level and constitutive biosynthesis of enantiopure germacrene D. The yeast strains developed in the present study might be useful for the microbial production of enantiopure germacrene D and other FPP-derived metabolites.

Supplementary Information The online version contains supplementary material available at https://doi.org/10.1007/s00253-023-12885-7.

Acknowledgements The authors gratefully acknowledge the Biological and Chemical Central Facility and Director, CSIR-CIMAP for research facilities. S. S., S. C., S. D acknowledge the CSIR for research fellowship. G. S. acknowledges the University Grants Commission for research fellowship. This manuscript has institutional communication no CIMAP/PUB/2023/89.

Author contribution S. S. developed CENses1-6 strains. S. C. developed CENses8 and CENses8* strains. A. S. developed CENses7 strain. S. S., S. C., S. D., and S. G. developed pESC and pYES2 constructs. S. S., S. C., G. S., and A. S. contributed in GC-FID analysis. S. S., S. C., and G. S. contributed in the GC–MS analysis. C. S. C. contributed in chiral GC-MS separation of compounds. S. C. and G. S. contributed in qRT-PCR. S. C. contributed in western blotting and growth curve analysis. S. G. contributed in codon optimization. All the authors contributed in experimental design and data analysis. S. G. conceived and coordinated the study and wrote the manuscript with inputs from S. S., S. C., G. S., and A. S. All the authors read and approved the final manuscript.

Funding S. G. received research grants from the Council of Scientific and Industrial Research (HCP-007 and MLP-19).

Data availability All the relevant data can be found within the article and the associated supporting information. The codon-optimized nucleotide sequences of *ScaGerD(+)*, *ScaGerD(−)*, *YlACL1*, and *YlACL2* were submitted in the NCBI GenBank database with accession numbers OR232701–OR232704. CENses8(+D) and CENses8(−D) strains were deposited in MTCC, India with accession numbers MTCC 25621 and MTCC 25622.

Declarations

Ethics approval This article does not contain any studies with human participants or animals performed by any of the authors.

Conflict of interest All the authors are inventors in a patent application arising from this work.

References

Adio AM (2009) Germacrenes A-E and related compounds: thermal, photochemical and acid induced transannular cyclizations. Tetrahedron 65(8):1533–1552. https://doi.org/10.1016/j.tet.2008.11.050

Asadollahi MA, Maury J, Møller K, Nielsen KF, Schalk M, Clark A, Nielsen J (2008) Production of plant sesquiterpenes in *Saccharomyces cerevisiae*: effect of ERG9 repression on sesquiterpene biosynthesis. Biotechnol Bioeng 99(3):666–677. https://doi.org/10.1002/bit.21581

Bröker JN, MüllerB PD, Schulze GC (2020) Combinatorial metabolic engineering in *Saccharomyces cerevisiae* for the enhanced production of the FPP-derived sesquiterpene germacrene. Bioengineering 7(4):135. https://doi.org/10.3390/bioengineering7040135

Bülow N, König WA (2000) The role of germacrene D as a precursor in sesquiterpene biosynthesis: investigations of acid catalyzed, photochemically and thermally induced rearrangements. Phytochem 55(2):141–168. https://doi.org/10.1016/s0031-9422(00)00266-1

Bureau JA, Oliva ME, Dong Y, Ignea C (2023) Engineering yeast for the production of plant terpenoids using synthetic biology approaches. Nat Prod Rep. https://doi.org/10.1039/d3np00005b

Cao C, Cao X, Yu W, Chen Y, Lin X, Zhu B, Zhou YJ (2022) Global metabolic rewiring of yeast enables overproduction of sesquiterpene (+)-valencene. J Agric Food Chem 70(23):7180–7187. https://doi.org/10.1021/acs.jafc.2c01394

Cascón O, Touchet S, Miller DJ, Gonzalez V, Faraldos JA, Allemann RK (2012) Chemoenzymatic preparation of germacrene analogues. Chem Commun 48(78):9702–9704. https://doi.org/10.1039/c2cc35542f

Casiglia S, Bruno M, Bramucci M, Quassinti L, Lupidi G, Fiorini D, Maggi F (2017) *Kundmanniasicula* (L.) DC: a rich source of germacrene D. J Essen Oil Res 29(6):437–442. https://doi.org/10.1080/10412905.2017.1338625

Chanotiya CS, Yadav A (2008) Natural variability in enantiomeric composition of bioactive chiral terpenoids in the essential oil of *Solidago Canadensis* L. from Uttarakhand, India. Nat Prod Commun 3(2). https://doi.org/10.1177/1934578X0800300232

Christianson DW (2017) Structural and chemical biology of terpenoid cyclases. Chem Rev 117(17):11570–11648. https://doi.org/10.1021/acs.chemrev.7b00287

Daum G, Tuller G, Nemec T, Hrastnik C, Balliano G, Cattel L, Milla P, Rocco F, Conzelmann A, Vionnet C, Kelly DE, Kelly S, Schweizer E, Schüller HJ, Hojad U, Greiner E, Finger K (1999) Systematic analysis of yeast strains with possible defects in lipid metabolism. Yeast 15(7):601–614. https://doi.org/10.1002/(SICI)1097-0061(199905)15:7%3c601::AID-YEA390%3e3.0.CO;2-N

Deng X, Shi B, Ye Z, Huang M, Chen R, Cai Y, Kuang Z, Sun X, Bian G, Deng Z, Liu T (2022) Systematic identification of *Ocimum sanctum* sesquiterpenoid synthases and (-)-eremophilene overproduction in engineered yeast. Metab Eng 69:122–133. https://doi.org/10.1016/j.ymben.2021.11.005

Dinday S, Ghosh S (2023) Recent advances in triterpenoid pathway elucidation and engineering. Biotechnol Adv 68:108214. https://doi.org/10.1016/j.biotechadv.2023.108214

Donald KA, Hampton RY, Fritz IB (1997) Effects of overproduction of the catalytic domain of 3-hydroxy-3-methylglutaryl coenzyme A reductase on squalene synthesis in *Saccharomyces cerevisiae*. Appl Environ Microbiol 63(9):3341–3344. https://doi.org/10.1128/aem.63.9.3341-3344.1997

Dulermo T, Lazar Z, Dulermo R, Rakicka M, Haddouche R, Nicaud JM (2015) Analysis of ATP-citrate lyase and malic enzyme mutants of *Yarrowia lipolytica* points out the importance of mannitol metabolism in fatty acid synthesis. Biochim Biophys Acta 1851(9):1107–1117. https://doi.org/10.1016/j.bbalip.2015.04.007

Engels B, Dahm P, Jennewein S (2008) Metabolic engineering of taxadiene biosynthesis in yeast as a first step towards Taxol (Paclitaxel) production. Metab Eng 10(3–4):201–206. https://doi.org/10.1016/j.ymben.2008.03.001

Faraldos JA, Wu S, Chappell J, Coates RM (2007) Conformational analysis of (+)-germacrene A by variable temperature NMR and NOE spectroscopy. Tetrahedron 63(32):7733–7742. https://doi.org/10.1016/j.tet.2007.04.037

Faulkner A, Chen X, Rush J, Horazdovsky B, Waechter CJ, Carman GM, Sternweis PC (1999) The LPP1 and DPP1 gene products account for most of the isoprenoid phosphate phosphatase activities in *Saccharomyces cerevisiae*. J Biol Chem 274(21):14831–14837. https://doi.org/10.1074/jbc.274.21.14831

Ghiffary MR, Prabowo CPS, Adidjaja JJ, Lee SY, Kim HU (2022) Systems metabolic engineering of *Corynebacterium glutamicum* for the efficient production of β-alanine. Metab Eng 74:121–129. https://doi.org/10.1016/j.ymben.2022.10.009

Gueldener U, Heinisch J, Koehler GJ, Voss D, Hegemann JH (2002) A second set of loxP marker cassettes for Cre-mediated multiple gene knockouts in budding yeast. Nucleic Acids Res 30(6):e23. https://doi.org/10.1093/nar/30.6.e23

Hu Y, Zhou YJ, Bao J, Huang L, Nielsen J, Krivoruchko A (2017) Metabolic engineering of *Saccharomyces cerevisiae* for production of germacrene A, a precursor of beta-elemene. J Ind Microbiol Biotechnol 44(7):1065–1072. https://doi.org/10.1007/s10295-017-1934-z

Jordá T, Puig S (2020) Regulation of ergosterol biosynthesis in *Saccharomyces cerevisiae*. Genes 11(7):795. https://doi.org/10.3390/genes11070795

Kim SR, Cha M, Kim T, Song S, Kang HJ, Jung Y, Cho JY, Moh SH, Kim SJ (2022) Sustainable production of shinorine from lignocellulosic biomass by metabolically engineered *Saccharomyces cerevisiae*. J Agric Food Chem 70(50):15848–15858. https://doi.org/10.1021/acs.jafc.2c07218

Kobayashi T, Heck DJ, Nomura M, Horiuchi T (1998) Expansion and contraction of ribosomal DNA repeats in *Saccharomyces cerevisiae*: requirement of replication fork blocking (Fob1) protein and the role of RNA polymerase I. Genes Dev 12(24):3821–3830. https://doi.org/10.1101/gad.12.24.3821

Kumar A, Srivastava P, Srivastava G, Sandeep KN, Chanotiya CS, GhoshS, (2021) BAHD acetyltransferase contributes to wound-induced biosynthesis of oleo-gum resin triterpenes in *Boswellia*. Plant J 107(5):1403–1419. https://doi.org/10.1111/tpj.15388

Labbé S, Zhu Z, Thiele DJ (1997) Copper-specific transcriptional repression of yeast genes encoding critical components in the

copper transport pathway. J Biol Chem 272(25):15951–15958. https://doi.org/10.1074/jbc.272.25.15951

Lian J, Si T, Nair NU, Zhao H (2014) Design and construction of acetyl-CoA overproducing *Saccharomyces cerevisiae* strains. Metab Eng 24:139–149. https://doi.org/10.1016/j.ymben.2014.05.010

Lin HH, Mendez-Perez D, Park J, Wang X, Cheng Y, Huo J, Mukhopadhyay A, Lee TS, Shanks BH (2022) Precursor prioritization for p-cymene production through synergistic integration of biology and chemistry. Biotechnol Biofuels Bioprod 15(1):126. https://doi.org/10.1186/s13068-022-02226-7

Liu J, Zhai Y, Zhang Y, Zhu S, Liu G, Che Y (2018) Heterologous biosynthesis of the fungal sesquiterpene trichodermol in *Saccharomyces cerevisiae*. Front Microbiol 9:1773. https://doi.org/10.3389/fmicb.2018.01773

Liu J, Chen C, Wan X, Yao G, Bao S, Wang F, Wang K, Song T, Han P, Jiang H (2022) Identification of the sesquiterpene synthase AcTPS1 and high production of (-)-germacrene D in metabolically engineered *Saccharomyces cerevisiae*. Microb Cell Fact 21(1):89. https://doi.org/10.1186/s12934-022-01814-4

Ma C, Zhang K, Zhang X, Liu G, Zhu T, Che Q, Li D, Zhang G (2021) Heterologous expression and metabolic engineering tools for improving terpenoids production. Curr Opin Biotechnol 69:281–289. https://doi.org/10.1016/j.copbio.2021.02.008

Ma Y, Zu Y, Huang S, Stephanopoulos G (2023) Engineering a universal and efficient platform for terpenoid synthesis in yeast. Proc Natl Acad Sci U S A 120(1):e2207680120. https://doi.org/10.1073/pnas.2207680120

Meadows AL, Hawkins KM, Tsegaye Y, Antipov E, Kim Y, Raetz L, Dahl RH, Tai A, Mahatdejkul-Meadows T, Xu L, Zhao L, Dasika MS, Murarka A, Lenihan J, Eng D, Leng JS, Liu CL, Wenger JW, Jiang H, Chao L, Westfall P, Lai J, Ganesan S, Jackson P, Mans R, Platt D, Reeves CD, Saija PR, Wichmann G, Holmes VF, Benjamin K, Hill PW, Gardner TS, Tsong AE (2016) Rewriting yeast central carbon metabolism for industrial isoprenoid production. Nature 537(7622):694–697. https://doi.org/10.1038/nature19769

Mockute D, Bernotiene G, Judzentiene A (2008) The essential oils with dominant germacrene D of *Hypericum perforatum* L. Growing Wild in Lithuania. J Essent Oil Res 20(2):128–131. https://doi.org/10.1080/10412905.2008.9699973

Noge K, Becerra JX (2009) Germacrene D, a common sesquiterpene in the genus Bursera (Burseraceae). Molecules 14(12):5289–5297. https://doi.org/10.3390/molecules14125289

Paddon CJ, Keasling JD (2014) Semi-synthetic artemisinin: a model for the use of synthetic biology in pharmaceutical development. Nat Rev Microbiol 12(5):355–367. https://doi.org/10.1038/nrmicro3240

Paddon CJ, Westfall PJ, Pitera DJ, Benjamin K, Fisher K, McPhee D, Leavell MD, Tai A, Main A, Eng D, Polichuk DR, Teoh KH, Reed DW, Treynor T, Lenihan J, Fleck M, Bajad S, Dang G, Dengrove D, Diola D, Dorin G, Ellens KW, Fickes S, Galazzo J, Gaucher SP, Geistlinger T, Henry R, Hepp M, Horning T, Iqbal T, Jiang H, Kizer L, Lieu B, Melis D, Moss N, Regentin R, Secrest S, Tsuruta H, Vazquez R, Westblade LF, Xu L, Yu M, Zhang Y, Zhao L, Lievense J, Covello PS, Keasling JD, Reiling KK, Renninger NS, Newman JD (2013) High-level semi-synthetic production of the potent antimalarial artemisinin. Nature 496(7446):528–532. https://doi.org/10.1038/nature12051

Peng B, Esquirol L, Lu Z, Shen Q, Cheah LC, Howard CB, Scott C, Trau M, Dumsday G, Vickers CE (2022) An in vivo gene amplification system for high level expression in *Saccharomyces cerevisiae*. Nat Commun 13(1):2895. https://doi.org/10.1038/s41467-022-30529-8

Prosser I, Altug IG, Phillips AL, König WA, Bouwmeester HJ, Beale MH (2004) Enantiospecific (+)- and (-)-germacrene D synthases, cloned from goldenrod, reveal a functionally active variant of the universal isoprenoid-biosynthesis aspartate-rich motif. Arch Biochem Biophys 432(2):136–144. https://doi.org/10.1016/j.abb.2004.06.030

Rana V S, Blázquez MA (2015) Essential oil composition of the aerial parts of five *Ocimum* species from western India. J Essent Oil-Bear Plants 18(5):1234–1241. https://doi.org/10.1080/0972060x.2014.931255

Rodriguez S, Kirby J, Denby CM, Keasling JD (2014) Production and quantification of sesquiterpenes in *Saccharomyces cerevisiae*, including extraction, detection and quantification of terpene products and key related metabolites. Nat Protoc 9(8):1980–1996. https://doi.org/10.1038/nprot.2014.132

Rodriguez S, Denby CM, Van Vu T, Baidoo EE, Wang G, Keasling JD (2016) ATP citrate lyase mediated cytosolic acetyl-CoA biosynthesis increases mevalonate production in *Saccharomyces cerevisiae*. Microb Cell Fact 15:48. https://doi.org/10.1186/s12934-016-0447-1

Schmidt CO, Bouwmeester HJ, Franke S, König WA (1999) Mechanisms of the biosynthesis of sesquiterpene enantiomers (+)- and (−)-germacrene D in Solidago canadensis. Chirality 11:353–362. https://doi.org/10.1002/(SICI)1520-636X(1999)11:5/63.0.CO;2-L

Sengupta S, Jana ML, Sengupta D, Naskar AK (2000) A note on the estimation of microbial glycosidase activities by dinitrosalicylic acid reagent. Appl Microbiol Biotechnol 53(6):732–735. https://doi.org/10.1007/s002530000327

Shi S, Valle-Rodríguez JO, Siewers V, Nielsen J (2014) Engineering of chromosomal wax ester synthase integrated *Saccharomyces cerevisiae* mutants for improved biosynthesis of fatty acid ethyl esters. Biotechnol Bioeng 111(9):1740–1747. https://doi.org/10.1002/bit.25234

Siemon T, Wang Z, Bian G, Seitz T, Ye Z, Lu Y, Cheng S, Ding Y, Huang Y, Deng Z, Liu T, Christmann M (2020) Semisynthesis of plant-derived englerin a enabled by microbe engineering of guaia-6,10(14)-diene as building block. J Am Chem Soc 142(6):2760–2765. https://doi.org/10.1021/jacs.9b12940

Srinivasan P, Smolke CD (2020) Biosynthesis of medicinal tropane alkaloids in yeast. Nature 585(7826):614–619. https://doi.org/10.1038/s41586-020-2650-9

Steliopoulos P, Wüst M, Adam KP, Mosandl A (2002) Biosynthesis of the sesquiterpene germacrene D in *Solidago canadensis*: 13C and (2)H labeling studies. Phytochem 60(1):13–20. https://doi.org/10.1016/s0031-9422(02)00068-7

Stranden M, Borg-Karlson AK, Mustaparta H (2002) Receptor neuron discrimination of the germacrene D enantiomers in the moth *Helicoverpa armigera*. Chem Senses 27(2):143–152. https://doi.org/10.1093/chemse/27.2.143

Stranden M, Liblikas I, König WA, Almaas TJ, Borg-Karlson AK, Mustaparta H (2003) (-)-Germacrene D receptor neurones in three species of heliothine moths: structure-activity relationships. J Comp Physiol A Neuroethol Sens Neural Behav Physiol 189(7):563–577. https://doi.org/10.1007/s00359-003-0434-y

Torchia TE, Hamilton RW, Cano CL, HopperJE (1984). Disruption of regulatory gene GAL80 in *Saccharomyces cerevisiae*: effects on carbon-controlled regulation of the galactose/melibiose pathway genes. Mol Cell Biol 4(8):1521–1527. https://doi.org/10.1128/mcb.4.8.1521-1527.1984

Valarezo E, Gaona-Granda G, Morocho V, Cartuche L, Calva J, Meneses MA (2021) Chemical constituents of the essential oil from ecuadorian endemic species *Croton ferrugineus* and its antimicrobial, antioxidant and α-glucosidase inhibitory activity. Molecules 26(15):4608. https://doi.org/10.3390/molecules26154608

van Rossum HM, KozakBU PJT, van Maris AJA (2016) Engineering cytosolic acetyl-coenzyme A supply in *Saccharomyces cerevisiae*: pathway stoichiometry, free-energy conservation and redox-cofactor balancing. Metab Eng 36:99–115. https://doi.org/10.1016/j.ymben.2016.03.006

Veen M, Stahl U, Lang C (2003) Combined overexpression of genes of the ergosterol biosynthetic pathway leads to accumulation of sterols in *Saccharomyces cerevisiae*. FEMS Yeast Res 4(1):87–95. https://doi.org/10.1016/S1567-1356(03)00126-0

Westfall PJ, Pitera DJ, Lenihan JR, Eng D, Woolard FX, Regentin R, Horning T, Tsuruta H, Melis DJ, Owens A, Fickes S, Diola D, Benjamin KR, Keasling JD, Leavell MD, McPhee DJ, Renninger NS, Newman JD, Paddon CJ (2012) Production of amorphadiene in yeast, and its conversion to dihydroartemisinic acid, precursor to the antimalarial agent artemisinin. Proc Natl Acad Sci U S A 109(3):E111–E118. https://doi.org/10.1073/pnas.1110740109

Yoshihara K, Ohta Y, Sakai T, Hirose Y (1969) Germacrene D, a key intermediate of cadinene group compounds and bourbonenes. Tetrahedron Lett 10(27):2263–2264. https://doi.org/10.1016/S0040-4039(01)88136-3

Zhang J, Hansen LG, Gudich O, Viehrig K, Lassen LMM, Schrübbers L, Adhikari KB, Rubaszka P, Carrasquer-Alvarez E, Chen L, D'Ambrosio V, Lehka B, Haidar AK, Nallapareddy S, Giannakou K, Laloux M, Arsovska D, Jørgensen MAK, Chan LJG, Kristensen M, Christensen HB, Sudarsan S, Stander EA, Baidoo E, Petzold CJ, Wulff T, O'Connor SE, Courdavault V, Jensen MK, Keasling JD (2022) A microbial supply chain for production of the anti-cancer drug vinblastine. Nature 609(7926):341–347. https://doi.org/10.1038/s41586-022-05157-3

Zhang W, Guo J, Wang Z, Li Y, Meng X, Shen Y, Liu W (2021) Improved production of germacrene A, a direct precursor of ß-elemene, in engineered *Saccharomyces cerevisiae* by expressing a cyanobacterial germacrene A synthase. Microb Cell Fact 20(1):7. https://doi.org/10.1186/s12934-020-01500-3

Zhao Y, Fan J, Wang C, Feng X, Li C (2018) Enhancing oleanolic acid production in engineered *Saccharomyces cerevisiae*. Bioresour Technol 257:339–343. https://doi.org/10.1016/j.biortech.2018.02.096